DESIGN, ASSEMBLY AND CALIBRATION OF AN EXPERIMENTAL SETUP FOR VARIOUS OPTICAL MEASUREMENTS

A THESIS SUBMITTED
TO
THE GRADUATE SCHOOL OF NATURAL AND APPLIED SCIENCES
OF
THE MIDDLE EAST TECHNICAL UNIVERSITY

BY

EVREN UZGEL

IN PARTIAL FULLFILLMENT OF THE REQUIREMENTS FOR THE DEGREE OF
MASTER OF SCIENCE
IN
THE DEPARTMENT OF PHYSICS

JANUARY 2004

Approval of the Graduate School of Natural and Applied Sciences

_____

Prof. Dr. Canan Özgen

Director

I certify that this thesis satisfies all the requirements as a thesis for the degree of Master of Science.

_____

Prof. Dr. Sinan Bilikmen

Head of Department

This is to certify that we have read this thesis and that in our opinion it is fully adequate, in scope and quality, as a thesis for the degree of Master of Science.

_____

Assoc. Prof. Dr. Gülay Öke

Supervisor

Examining Committee Members

Prof. Dr. Sinan Bilikmen _____

Assoc. Prof. Dr. Akif Esendemir _____

Assoc. Prof. Dr. Gülay Öke _____

Assoc. Prof. Dr. Serhat Çakır _____

Dr. Ali Alaçakır _____

ABSTRACT

DESIGN, ASSEMBLY AND CALIBRATION OF AN EXPERIMENTAL SETUP FOR VARIOUS OPTICAL MEASUREMENTS

Uzgel, Evren

M.S., Department of Physics
Supervisor: Assoc. Prof. Dr. Gülay Öke

January 2004, 50 pages

The experimental setup which consisted of the Jarrell-Ash Ebert type scanning monochromator, the Hamamatsu Si PIN Photodiode, a PC connected ADC card and a Tungstenstriplamp operated at different temperatures was assembled. The different parts needing calibration were calibrated with spectral response calibration techniques suitable for our purposes and connected to the experimental setup in a proper way. Spectral response calibrations and transmission measurements in the range 450-800 nm were carried out.

Keywords: Spectral response calibration, Transmission coefficient, Monochromator, Photodiode

ÖZ

FARKLI OPTİK ÖLÇÜMLER İÇİN BİR DENEY KONFİGÜRASYONUNUN DİZAYNI, BİRLEŞTİRİLMESİ VE KALİBRASYONU

Uzgel, Evren

Yüksek Lisans, Fizik Bölümü
Tez Yöneticisi: Doç. Dr. Gülay Öke

Ocak 2004, 50 sayfa

Jarrell-Ash Ebert tipi tarama monokromatör ünitesi, Hamamatsu Si PIN Photodiode , PC bağlantılı ADC kartı ve farklı sıcaklıklarda kullanılan Tungsten lambasından oluşan deney konfigürasyonu oluşturulmuştur. Kalibre edilmesi gereken farklı parçalar amacımıza uygun spektral duyarlılık kalibrasyon teknikleriyle kalibre edilmiş ve deney konfigürasyonuna uygun bir biçimde monte edilmiştir. 450-800 nm aralığında spektral duyarlılık kalibrasyonu ve transmisyon ölçümleri yapılmıştır.

Anahtar kelimeler: Spektral duyarlılık kalibrasyonu, Transmisyon katsayısı, Monokromatör, Fotodiod

ACKNOWLEDGEMENTS

I would like to thank Assoc. Prof. Dr. Gülay Öke, Assoc. Prof. Dr. Akif Esendemir and Dr. Ali Alaçakır for their knowledgeable support ,encouragement and for their useful advices and technical support involving methods and instruments used in the experiment.

TABLE OF CONTENTS

CHAPTER 1
INTRODUCTION

During plasma operation optical components like windows, mirrors and lenses can be coated and will change their transmission and reflection coefficients. Therefore the spectral dependence of the optical components must be determined. The relative calibration is sufficient for many applications to investigate the dependence of different plasma parameter, but for determination of some plasma parameter also absolute photon fluxes have to be measured.

The aim of the master thesis is the design, assembly and calibration of an optical setup that allows the determination of the transmission and reflection coefficients of optical components within the wavelength range from 450 nm to 800 nm. Calibrated light sources which are covering the proposed wavelength range are illuminating the entrance slit of a monochromator. The selected small wavelength range at the entrance slit is transferred into a parallel light beam that passes or hits the probing optical component. The reflected light is focussed into a calibrated detector. The wavelength is scanned by rotation of the dispersive element in the monochromator. The ratio of the measured curves with and without the tested optical component delivers the transmission or reflection coefficients.

Design, assembly and calibration of the experimental setup and calibration are the three main subjects of this thesis.

Design considerations involve the determination and compatibility of the optical instrumentation. In our case an Ebert type monochromator is coupled with a Si PIN Photodiode while using a tungsten strip lamp as the radiation standard giving us a setup suited for carrying out transmission measurements and spectral response calibrations of different optical parts.

The possible choices of optical detectors and multiple electronic devices that detect optical radiation and for which the output is in electrical rather than optical form are discussed where the most interesting one of these devices for our case is the Si PIN Photodiode. The working principle, different applications and the spectral response of various photodiodes is given. For the scan of various wavelengths an Ebert type monochromator is chosen and basic knowledge about it is provided. The calibration data of the tungsten strip lamp is included. The technical specifications of the assembled parts are given.

Calibration of optical instrumentation is discussed and the techniques most suitable for our setup are determined. Angular response, and Spectro-angular response calibration is of no interest to us since the light source doesn't move, the slits of the monochromator permit only the irradiation of a distinct area of the Si PIN Photodiode active area and the diffraction grating of the monochromator reflects only one wavelength at a time on the Si PIN photodiode which is also the essential sense of the monochromator. Spectral response calibration of the monochromator and Si PIN Photodiode can be carried out which will permit spectral response calibration of other optical instrumentation.

Multiple difficulties have been encountered during each stage namely the design, assembly and calibration of the setup. The most important of all being the absence of a device able to measure the diodeoutput in terms of current. While considering the design of the setup, availability of the parts which were already at hand,the lack of corresponding manuals and incredible shipping times for various parts ordered from different countries were a major issue. Assembling the different parts presented difficulties such as different spectral response regions and electronic compatibility.

CHAPTER 2
DESIGN CONSIDERATIONS

2.1 CHOICE OF OPTICAL DETECTOR

The ultimate detector of optical waves is the eye.Detectors of optical radiation by electronic devices, for which the output is in electrical rather than optical form are relevant to our case.

Optical detectors can be classified in many ways: by how they work; by the optical spectrum to which they are sensitive; whether they are passive or active; whether they exhibit gain; whether the gain is photonic or electronic; whether they are thermionic or semiconductor devices; and whether they are direct energy converters or energy controllers. We may determine whether they are noisy or not.

A brief examination of different types of detectors will be necessary to determine some of the detectors suited for our purpose.

2.1.1 Types of detectors

Most optical detectors use direct or indirect energy conversion from input optical energy into output electrical energy. The archetype of such detectors is the photovoltaic diode, which closely resembles the solar cell, except that in the solar cell the device is designed to have a broad band response and the prime design consideration is efficient energy conversion. Photodiodes are semiconductor light sources that generate a current or voltage when the P-N junction in the semiconductor is illuminated by light.

The semiconductor photodiode is a pn junction designed to absorb photons in a region close to the junction. The PIN Photodiode consists of an intrinsic layer between the P-N junction having the advantage of an extended spectral response region, low capacitance and higher frequency operation. The detector used in the setup is a Si PIN Photodiode.

There are other detectors which, whilst accepting the input energy in optical form and delivering output energy in electrical form, employ an intermediate step in which the optical energy is converted into another energy form before conversion into electrical energy.

Foremost of these hybrid detectors is the pyroelectric detector. The inefficiency of using an intermediate energy state means that whilst this device is robust and simple it cannot compete with other detectors in sensitivity. Consequently the pyroelectric detector is used only in the less demanding role of low sensitivity monitoring.

Another example is the thermoelectric energy converter in which the input energy is converted into heat at a thermo-junction and this heat is converted into electrical energy by the thermoelectric effect. This process has had limited success in the solar energy field, but as a photodetector it is not competitive with direct energy converting detectors.

A third category of detectors are those in which the absorbed optical energy is used to control the energy in an external electrical circuit. The principle contenders in this category are the photoconductive detector, the reverse biased photodiode, the photomultiplier, and the avalanche detector.

In the photoconductive detector a bulk semiconductor absorbs the incident radiation with a consequent generation of holes and electrons. Unlike the energy conversion devices, the number of electrons traveling around the external circuit is no longer limited to one per photon, so that *amplification* is possible.

The reverse biased photodiode also offers amplification of the photovoltage by developing the incremental photocurrent through the large reverse resistance of the cell.

The photomultiplier is a cold cathode detector that amplifies the photocurrent arising from the energy absorption at the cathode by accelerating the

emitted electrons to produce secondary emission from a high potential anode.

The solid state equivalent of the photomultiplier is the avalanche diode in which an amplified photocurrent is achieved by operating a reverse biased diode near its reverse voltage limit where avalanche current conditions prevail.

2.2 THE PHOTODIODE

2.2.1 Principle of operation

The P-layer material at the active surface and the N material at the substrate form a PN junction which operates as a photoelectric converter.

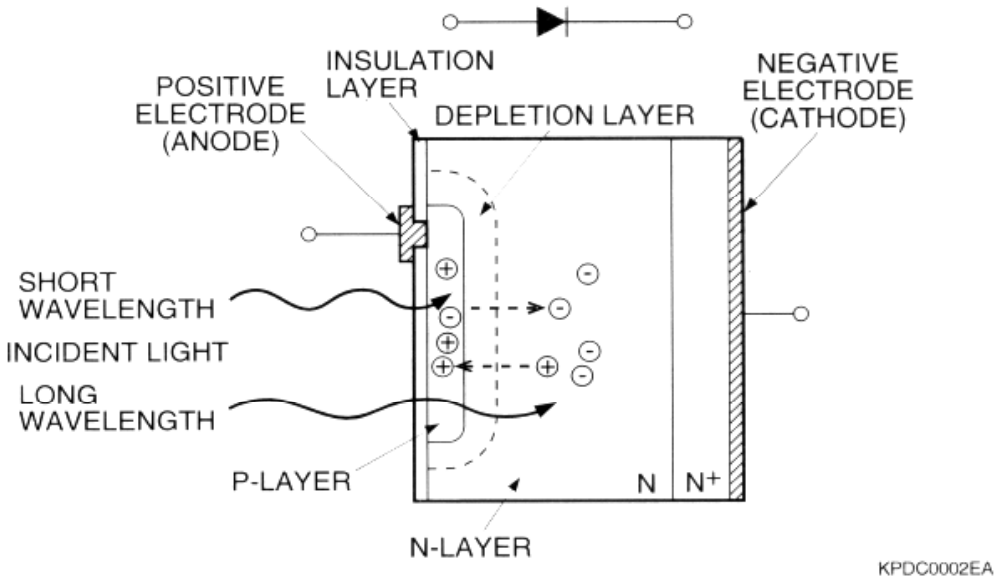

Figure 1 photodiode cross section [16]

The usual P-layer for a Si photodiode is formed by selective diffusion of boron, to a thickness of approximately 1μm or less and the neutral region at the junction between the P- and N-layers is known as the depletion layer. By

controlling the thickness of the outer P-layer, substrate N-layer and bottom N^+-layer as well as the doping concentration, the spectral response and frequncy response can be controlled. When light strikes a photodiode, the electrons within the crystal structure becomes stimulated. If the light energy is greater than the band gap energy E_g , the electrons are pulled up into the conduction band, leaving holes in their place in the valance band.

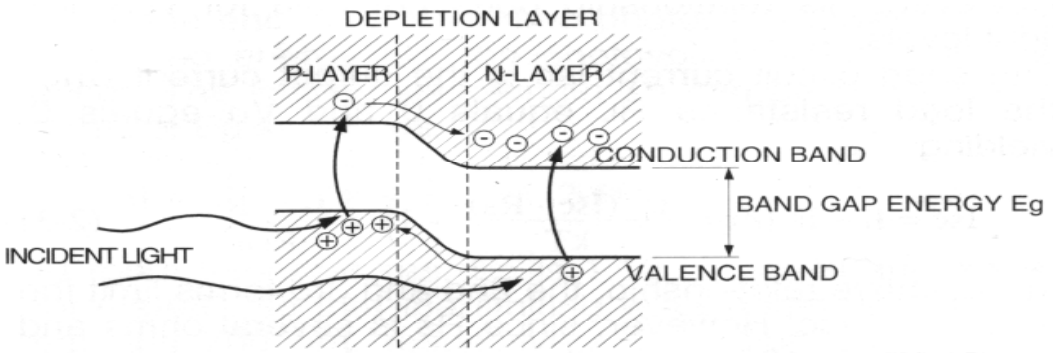

Figure 2 Photodiode P-N junction state [16]

These electron-hole pairs occur throughout the P-layer, depletion layer and N-layer materials. In the depletion layer the electric field accelerates these electrons toward the N-layer and the holes toward the P-layer. Of the electron-hole pairs generated in the N-layer, the electrons, along with the electrons that have arrived from the P-layer, are left in the N-layer conduction band. The holes at this time are being diffused through the N-layer up to the depletion layer while being accelerated, and collected in the P-layer valence band. In this manner, electron-hole pairs which are generated in proportion to the amount of incident light are collected in the N- and P-layers. This results in a positive charge in the P-layer and a negative charge in the N-layer. If an external circuit is connected between the P- and N-layers, electrons will flow away from the N-layer, and holes will flow away from the P-layer toward the opposite respective electrodes. These electrons and holes generating a current flow in a semiconductor are called the carriers.

2.2.2 The PIN Photodiode

The desire to operate with low capacitance and with an extended region in which holes and electrons can be generated has led to a modification of the simple PN structure photodiode, with the inclusion of an intrinsic region between P- and N- layers. Photodiodes operating according to this structure are called PIN photodiodes. The presence of an extended intrinsic region leads to lower capacitance compared to PN photodiodes and decreases the time required to respond to a change of photon flux although the transit time from one depletion region to the other increases.

2.3 THE OPERATINGWAVELENGTH AND TEMPORAL RESPONSE OF PHOTODETECTORS

2.3.1 The operational wavelengths of photodetectors

Whatever the type of photodetector the response of the detector is governed by the energy band structure in the active photon absorption region of the detector. The absorption may lead to the creation of thermal energy, as in the case of hybrid detectors using optical-thermal-electrical energy conversion. For direct optical-electrical energy converters the photon absorption leads to the freeing of charge carriers or the creation of charge carrier pairs, the movement of which constitute an electric current. For photon absorption to occur there must be unoccupied electron energy levels above occupied electron energy levels with the spacing equal to hc/λ .For pn devices, the photon energy must exceed the band-gap energy which means that operation is limited to free space wavelengths less than *hc/Eg.* In practice semiconductor photodiode are operated close to *hc/Eg,* to avoid the loss of efficiency that accompanies excessive absorption outside the immediate vicinity of the junction. [5]

2.3.2 The temporal response of photodetectors

The speed of photodetectors response is a vital measure of their usefulness in high-speed optical circuits. The four principal factors that limit temporal response are the intrinsic capacitance, the transit time delays, the diffusion time and the physical dimensions. It is desirable to keep physical dimensions small to minimise the effect of the inductance of connecting leads. This eliminates bulky devices such as photo-multipliers when seeking very fast response. Capacitive and transit time delay effects are additive and, as we have seen with the pin diode, attempts to reduce the diode capacitance may increase transit time delay, so that a device design minimising the total delay from the two sources is necessary. Diffusion times can be minimised by ensuring that absorption occurs very close to the depletion region. [11]

2.4 THE NOISE PERFORMANCE OF PHOTODETECTORS

The inevitable natural noise is the thermal noise present in a conductor at any temperature above absolute zero. In addition the photodetector adds its own self-generated noise, which will reduce the *detectability* of the received signal.

2.4.1 Thermal noise

Thermal noise is due to the random currents that occur in a conductor as a consequence of its thermal environment. If the absolute temperature of a conducting media ***T,*** and the resistance between two points in the medium ***R,*** is known the mean square random voltage observed between the two points due to the thermal environment can be found. This result is central to determining the rate at which information can be transmitted in a thermal environment, and

provides a reference against which to measure observed noise in real systems.

The principle source of noise in photodetectors is shot noise, which is observed in all electronic devices. Shot noise arises because of the discrete nature of the current flow in all electronic devices. In the semiconductor photodiode, for example, the shot noise arises as a consequence of the discrete generation of hole-electron pairs in the depletion region, which can of course be traced back to the discrete nature of photon events in the photon flux that causes the carrier generation. The presence of shot noise places a fundamental limitation on the sensitivity of the detector in the context of the system in which it is embedded.

2.5 THE MONOCHROMATOR

The monochromator is an optical instrument used widely in many optical experiments concerning spectrometry. The simple but useful idea of the monochromator is that it enables us to analyze a distinct wavelenght of the spectrum at hand making it very useful for spectral response calibrations. Light enters through the entrance slit and passes to a concave mirror, where it is collimated and reflected as parallel light to a plane grating. The dispersed light, still parallel, but with separate wavelenghts diverging, is reflected back to the mirror. There the light is again reflected and focused as monochromatic light at the exit slit. The wavelength of monochromatic light emerging at the exit slit is changed by simply rotating the grating about its center. The entrance and exit slit heights and widths can be varied and the source chopped or unchopped. The light can be focused directly at the entrance slit or predispersed through a prism. Prefiltering at the longer wavelengths is accomplished with band-pass interference filters.

2.5.1. The Diffraction Grating:

The diffraction grating consists of a number of straight, equidistant parallel grooves ruled on a plane or concave optical surface in order to take advantage of the diffraction of the incident light to analyze distinct wavelengths at the exit slit. Classically ruled gratings, which are used in the setup, are manufactured by cutting groove after groove into a substrate with a diamond tool. Echelle and holographic gratings are also used for different wavelength and resolution requirements. Blaze wavelength, resolution, groove density, dispersion and spectral range are used to characterize the diffraction grating. The blaze wavelength is the wavelength at which the grating is at its maximum efficiency. Groove density is the number of grooves per mm on the grating surface. The useful range of a grating can be conveniently described by the 2/3-3/2 rule which simply gives the range of a grating to be lower limit=2/3 of blaze wavelength; upper limit=3/2 of blaze wavelength. The resolution of the grating describes its ability to produce distinct peaks for closely spaced wavelengths in a particular order. Dispersion is a measure of the angular separation per unit range of wavelength.

CHAPTER 3
ASSEMBLY OF THE SETUP

3.1 THE JARRELL-ASH EBERT TYPE MONOCHROMATOR

The Jarrell-Ash scanning monochromator used in the setup is of Ebert type with a motor driven grating that also allows manual operation. An advanced version of the Jarrell-Ash scanning monochromator the Monospec 50 (Model 82-049) is also present at our laboratories .The focal length of the monochromators is 0.5 m. The effective aperture ratio is given as f/8.6. The specifications for the gratings used in the setup are: 1200 g/mm, 500 nm blaze wavelength, 300-1100 nm spectral range, 1.6 nm/mm reciprocal linear dispersion, 0.02 nm resolution in the first order[17]; 1180 g/mm, 600 nm blaze wavelength, 400-1200 nm spectral range, 1.6 nm/mm reciprocal linear dispersion, 0.02 nm resolution in the first order[17]. The efficiency curves of the gratings with respect to wavelength could not be obtained from the manufacturer due to the relative old age of the gratings and the stubborness of the manufacturer. The entrance and exit slits are adjustable in the range 0-2000 μm. The grating is mounted and leveled in a pivot. It is rotated by action of a lever arm, fastened to the lower end of this pivot and driven by a nut and precision screw. The linkage is designed to provide a motion linear with the sine of the angle of rotation. This enables the screw rotation to remain directly proportional to the wavelength. An instrument performance check was carried out and most parts of the monochromator were found to be working properly. The wavelength calibration was done simply by adjusting the grating tilt screws. Optical alignment of the system was checked with the help of a laser. The laser beam entering through the entrance slit stroke exactly the center of the grating after manipulation of the mirror adjustment screws. Grating tilt and level

adjustments were done using a mercury lamp and checking the image at the exit slit relative to the entrance slit.

3.2 THE HAMAMATSU Si PIN PHOTODIODE:

The Hamamatsu Si PIN Photodiodes S1133-14(320-1000 nm spectral response range, 720 nm peak sensitivity wavelength, 10 pA max dark current) [16], S1227-33BQ(190-1000 nm spectral response range, 720 nm peak sensitivity wavelength, 30 pA max dark current) [16], S2506-02(320 to 1100 nm spectral response range, 960 nm peak sensitivity wavelength, 100 pA max dark current) [16]. Common applications of these photodiodes are spatial light transmission, optical switches, optical measurement, display light control and laser radar. The most obvious advantages of these photodiodes:

Excellent linearity with respect to incident light, low noise, wide spectral response, mechanically rugged, compact and lightweight, long life.

The specifications of different types of the Si PIN Photodiodes are given below:

■ General ratings / Absolute maximum ratings

Type No.	Dimensional outline	Package	Active area size (mm)	Effective active area (mm^2)	Absolute maximum ratings: Reverse voltage V_R Max. (V)	Power dissipation P (mW)	Operating temperature Topr (°C)	Storage temperature Tstg (°C)
S2506-02	①	Plastic	2.77 × 2.77	7.7	35	150	-25 to +85	-40 to +100
S2506-04								
S6786								
S6967	②		5.5 × 4.8	26.4		50		
S6967-01								

■ Electrical and optical characteristics (Typ. Ta=25 °C, unless otherwise noted)

Type No.	Spectral response range λ (nm)	Peak sensitivity wavelength λp (nm)	Photo sensitivity S (A/W) λp	660 nm	780 nm	830 nm	Short circuit current Isc 100 lx (μA)	Dark current ID Typ. (nA)	Dark current ID Max. (nA)	Temp. coefficient of ID T_{CID} (times/°C)	Cut-off frequency fc R_L=50 Ω -3 dB (MHz)	Terminal capacitance Ct f=1 MHz (pF)	NEP (W/$Hz^{1/2}$)
S2506-02	320 to 1100	960	0.56	0.4	0.48	0.5	7.3	0.1 *1	10 *1	1.15	25 *1	15 *1	1.0 × 10^{-14} *1
S2506-04	760 to 1100			-	-	0.25	4.1						
S6786	320 to 1060	900	0.65	0.45	0.55	0.6	7.5	0.3 *2	5 *2		60 *2	15 *2	1.5 × 10^{-14} *2
S6967							26	0.5 *2			50 *2	50 *2	2.0 × 10^{-14} *2
S6967-01	700 to 1060		0.63	-	0.48	0.54	18						

*1: V_R=12 V
*2: V_R=10 V

SOLID STATE DIVISION

Figure 3 Characteristics of PIN photodiodes [16]

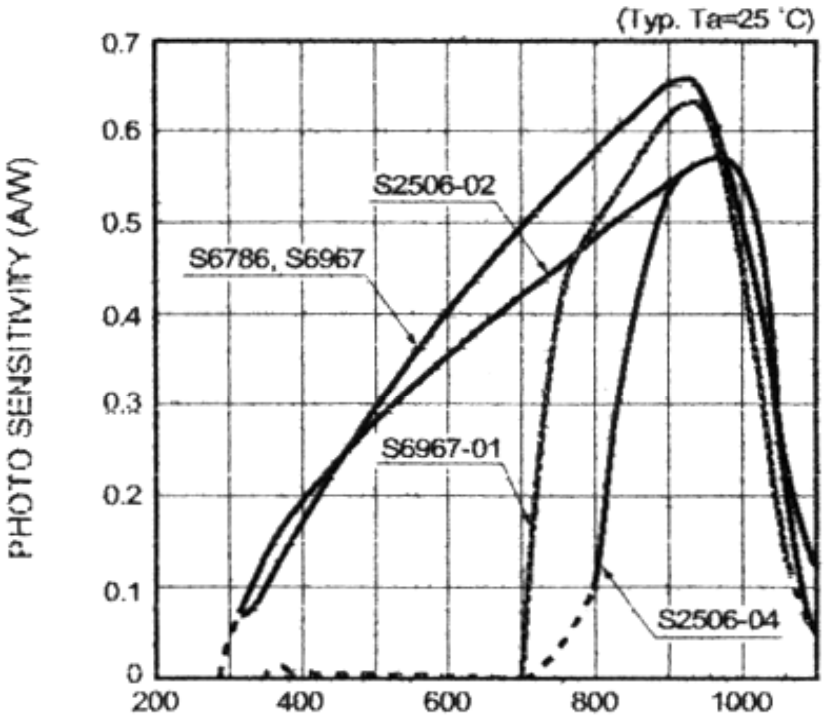

Figure 4 Spectral responses of PIN photodiodes [16]

3.3 THE OSRAM TUNGSTEN LAMP:

The tungsten filament lamp is the most popular source for optical instrumentation designed to use continous radiation in the visible and into the infrared region. The filament is in ribbon form which is contained in a glassbulb. Knowing the spectral emissitivity and the temperature of the ribbon one can calculate the spectral radiant exitance and the spectral dependence of the absolute photon flux which is essential in determining the transmission and reflection coefficients. The calibration of the lamp has been done by Mr. Cremerius at the FZ-Juelich by means of a precision-micro-pyrometer. The dependence of the temperature of the ribbon with respect to the heating current flowing through the lamp and with respect to the supply voltage were measured simultaneously. The calibration data is given below.

Kelvin	Volt	Ampere
2400	7,55	13,02
2500	8,61	13,96
2600	9,68	14,87
2700	10,92	15,96

Figure 5 Calibration data of tungsten strip lamp

CHAPTER 4
CALIBRATION TECHNIQUES

4.1. INTRODUCTION

The purpose of detector calibration is usually to gather sufficient information about the performance characteristics of the sensor to convert its output to a desired FIELD radiometric quantity [14]. A FIELD quantity is one that exists in space independent of any instrument one might place there to measure it. The complexity of the scene that will irradiate the sensor during measurement determines to a large extent what calibration procedures must be performed. If, for example, it is known that the source is a small, nearly monochromatic one, the calibration may consist only of irradiating the sensor with a standard source of that type at the anticipated angle of incidence and to neglect the fact that the sensor would respond differently for other wavelengths and other angles of incidence. In our setup the angle of incidence doesn't change with time or with the wavelenght because of which the angular and spectro-angular calibration isn't required.

The spectral calibration of grating monochromators is achieved by using suitable standard light sources like calibrated gas discharge lamps, carbon arcs, synchrotron radiation etc. The tungsten strip lamp is suited for the visible and near-infrared region where the near-uv region presents a problem because of the lamps rapidly decreasing emissitivity towards lower wavelengths.

4.2. SENSOR RESPONSE DEFINITIONS

Radiometric sensors in general respond neither as omnidirectional receivers nor according to a simple cosine law; a reasonably good analogy might be that they are equivalent to surfaces having spectrally selective topographical features [9]. In order to interpret the output of a sensor it is often necessary therefore to measure its *spectro-anqular* response characteristics.

4.2.1. Spectral Response

For many practical applications it is necessary to measure the sensor spectral response at only one angle of incidence. If, for example, the source is a small stationary one at a large distance such that the sensor aperture subtends a small solid angle at the source and vice-versa, the variation of sensor response with angle of incidence is irrelevant. It would be sufficient to irradiate the sensor with the collimated output of a monochromator at the same angle of incidence as that which will exist at the time of the measurement and then to scan the monochromator in wavelength while recording the sensor output.

4.2.2. Angular Response

It is sometimes valid to base the angular response calibration on a single field-of-view map at a fixed monochromator setting λ_k. A typical example is a small field-of-view sensor designed to isolate a spectral ”line” of a source that is too extensive to satisfy the small-source criteria . It is also assumed that there is no significant change in spectral response within the small angular region involved.

4.2.3. Spectro-Angular Response

If the source is both spectrally broad and large it often is necessary to map the sensor response as a function of both wavelength and angle of' incidence. The symbol for the sensor spectro-angular response is $S(\theta,\varphi,\lambda_k)$ which is everywhere less than or equal to unity. The usual procedure is to design the experiment in such a manner that the spectral and angular responses are independent. The calibration time is thus greatly reduced and the precision of the ensuing measurement is greatly enhanced.

4.3 SPECTRAL RESPONSE CALIBRATION

4.3.1 The Monochromator System

The monochromator can be used for various calibrations of detectors as it offers different kinds of applications by enabling the installation of various instrumentation like beamsplitters, choppers, lock-in amplifiers etc.

The calibration of a detector for example contains a beamsplitter slotted fixture and a twoposition chopper fixture at the exit slit that can be used to chop the exit radiation at either or both exits. For certain applications a standard, calibrated detector is placed at one of the exits and the sensor to be calibrated is placed at the other exit. Since the spectral transmittance and reflectance characteristics of the beamsplitter are known, that approach allows real-time monitoring of the spectral irradiance at the aperture of the sensor being calibrated. For other applications, the beamsplitter is removed and sequential monochromator scans are performed, irradiating the standard detector during one scan and then the sensor in a subsequent scan. The sequential approach is not as good as the real-time approach but is sometimes necessary because of interface problems. It is subject to error if the source is not stable and therefore requires frequent checks on the stability of the source.

It is not possible to perform angular response scans with the monochromator in our setup set at a fixed wavelength: however, new monochromators are interfaced with angular response systems so that angular scans at fixed monochromator wavelength settings can be performed.

4.3.2 Order Effects and Stray Radiation Effects

As is the case in all calibration procedures, the sensor ouput due to the source must be determined during spectral response calibrations for which the source of interest is a narrow band of radiation centered at the monochromator readout wavelength λ_m**.** In addition to that spectral "line," higher-order lines at wavelengths λ_m/n, where *n* is an integer, are also present at the exit slit of a grating monochromator for a given monochromator setting. The irradiance due to those lines can be reduced to negligible values by prefiltering. A convenient prefiltering technique is to place a long-wavelength pass filter or "order sorter" at the monochromator entrance slit. The transmittance characteristics of some typical order sorters are commercially available from colored-glass manufacturers. Order sorting can also be accomplished by a predispersing prism.

In addition to order effects, the monochromator output also contains an irradiance component that might be lumped under the heading of "stray radiation." The stray radiation component can contain, among other things, radiation scattered undispersed to the exit slit and, at longer wavelengths, radiation emitted by the monochromator and the environment in which the calibration is performed. Although it is usually a simple matter to eliminate order effects, the elimination of stray radiation is often difficult to accomplish. Frequently it is necessary to accept the stray radiation component as a necessary evil and to subtract its contribution from the sensor output to arrive at the true spectral irradiation. A frequently used method is to set the monochromator to some very short or very long wavelength λ_m where it is known that the irradiance at that wavelength is too small to stimulate the sensor; the sensor output obtained under those conditions is usually a good approximation to the stray radiation

component. Stray radiation effects can be reduced by the use of double-pass monochromators and by band-pass filters, if available.

4.3.3 Detector Spectral Response Calibration

The measurement of the spectral response of a radiometer is, in principle a simple procedure. All that is required is to compare the radiometer true spectral radiation values with those of a standard radiometer of known spectral response as the monochromator is scanned in wavelength. The absolute spectral sensitivity of the Si PIN Photodiode used in the setup is known a priori from the catalog of the supplying firm.

4.3.4 Spectrometer Spectral Response Calibration

When a monochromator is used to measure the spectral resolution elements of a spectrometer it is set at a fixed wavelength while the spectrometer scans. If one is interested in measuring the true spectral irradiance at only a few λ values, it is often more convenient to use a spectral "line" source such as a Hg lamp or a laser. In neither case is it necessary to determine the absolute value of the spectral irradiance since all true spectral radiation values obtained during a spectrometer scan are normalized to the peak value. For most spectrometers, the spectral resolution element does not vary significantly over a large portion of the spectral region to which they respond [6].

Although the measurement of the spectral response of a radiometer and the spectral resolution element of a spectrometer require a monochromator, the measurement of the spectrometer spectral response can be performed using a broadband source, usually a blackbody.

CHAPTER 5
EXPERIMENTAL PROCESS

5.1 SETUP CHARACTERISTICS:

Important factors that limited the accuracy and range of the data taken are: the resolution of the monochromator nearly equalling 1.5 nm for full slitwidth, the sensitivity of the ADC card which can only be calibrated down to the mV range, the apparent incompatibility between the diodes and the ADC card, the lack of a device able to measure the diodes output in terms of Amperes since the outputcurrent is in the range of nA, the multiplication of noise because of the large resistance attached to the diode, deposited tungsten on the inner bulb surface which can decrease the flux output by as much as %18 [7] and the relative low transmittance of the glass bulb of the tungsten strip lamp below 400nm. The dark current of the photodiodes can't be detected by the ADC card but can be estimated to be 1 mV when compared with measurements done by other instruments.

The temperature dependence of the photodiodes is negligible relative to the factors above. The power supply of the lamp provided the exact values required for the operation at distinct ribbon temperatures and the voltage and current values didn't vary from the determined values of the calibration curve of the lamp. The average efficiency of Ebert type monochromators varies between 0.96 and 0.97 [18] in the region from 450nm to 800nm and is also negligible. The efficiency curves of the diffraction gratings are unknown. Stray light contributions and order effects have also been neglected. Diffraction and interference arising from the slits are of no concern since the slitwidth is $2*10^{-3}$m where the wavelength is in the 10^{-6} m range.

The threshold of the setup lies at 450nm meaning that below this value the diodeoutput isn't significantly larger than the noise of the system and is subject to serious variations. The incompatibility of the ADC card and the diodes manifests itself in the manner that the diodeoutput varies constantly about 2 mV at a fixed wavelength when measured with the ADC card; but only shows variation equal to the internal noise of equipment like digital multimeters and oscilloscopes when measured with those. The other sign of incompatibility is that if no light is incident on the active area of the diodes the digital multimeter and the oscilloscope read a diodeoutput of nearly 0 mV whereas the ADC card reads values between -300 mV and 300 mV with no apparent waveform or frequency!

Observable factors that affect the output of the Hamamatsu Si PIN Photodiodes are: the distance of the light source from the entrance slit, the temperature of the tungsten ribbon, the wavelengh, the value of the resistance attached to the diode and the widths of the entrance and exit slits. Increasing the distance of the light source, reducing the widths of the slits will lead to a drop in output and vice versa. The fluctuations of the diodeoutput measured with the ADC card are greater for the 450nm-500nm range where a more rapid increase in diodeoutput is observed compared to the 500nm-800nm range.

5.2 EXPERIMENTAL PROCEDURE AND DATA:

5.2.1 Aim of the procedure:

The aim of the setup is to determine the spectral dependence of the absolute photon flux of the calibrated lamp, calibrate the diode in terms of its spectral sensitivity by comparison to the photon flux of the calibrated lamp; thus being able to determine the spectral dependence of the photon flux of any light source or the spectral sensitivity of any detector implemented in to the system. The ratio of the measured curves with and without the optical component in front of the exit slit will give us simply the transmission coefficient of the component

with respect to the wavelength from which we can deduce the reflection coefficient of the component with respect to the wavelength.

5.2.2 Method and Specifications:

The configuration of the parts doesn't change during the data acquisition process. The only dynamic part is the grating which can be set to scan speeds of 500, 250, 125, 50 A^0/min or manual for the old monochromator and between 200 to 2000 A^0/min for the Monospec 50[17]. The spectra of the lamp is obtained between 450-800 nm wih scanning speeds of 500 A^0/min and 2000 A^0/min for the old and new monochromator respectively, to counter the low resolution of the grating. The distance of the tungsten strip to the entrance slit was 7 cm. The slitwidth was 2mm. The active area of the photodiode was completely exposed to the incident light. The temperatures of the tungsten ribbon was set to 2600K and 2700K respectively. All data and graphics presented in this chapter are for the S2506-02 Si PIN photodiode.

Since the PIN photodiode does generate a power due to the photovoltaic effect, it can operate without the need for an external power source. Keeping that in mind the leads of the diode were connected directly to the ADC card which acts as a voltmeter (which leads to the assumption of a constant ohmic internal resistance). The outputsignal in V should be directly proportional to the photocurrent where the internal resistance of the ADC card has to be the proportionality constant. The resulting data was between 10mV to 220MV with serious drops between 45nm-500nm, had serious fluctuations and inconsistencies between successive data sets which led to the pursuation of alternative methods.

The second method was to construct the circuit for Si PIN photodiodes depicted in the manufacturer's cathalog, to increase linearity and allow amplification of the outputsignal, as shown in the figure below.

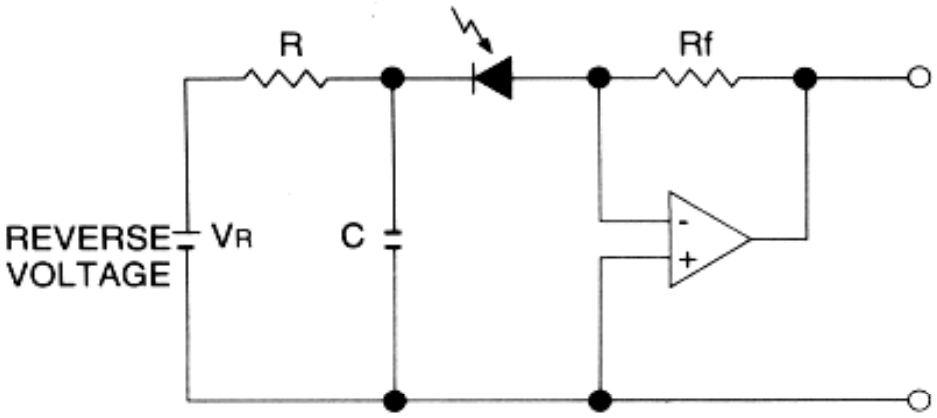

Figure 6 Reverse voltage connection circuit for PIN photodiodes [16]

Where R=1 KΩ, V_R=12 V, C=100 nF-20nF and Rf was a reosta between 100Ω-100KΩ which are all values recommended by the manufacturer or by various books on electronic devices. The resulting data was between 1mV to 25mV and had serious noise and fluctuations in the 3mV range due to the amplification.

The final method was to connect a resistance in series to the leads of the diode and connect the ADC card parallel to the resistance.

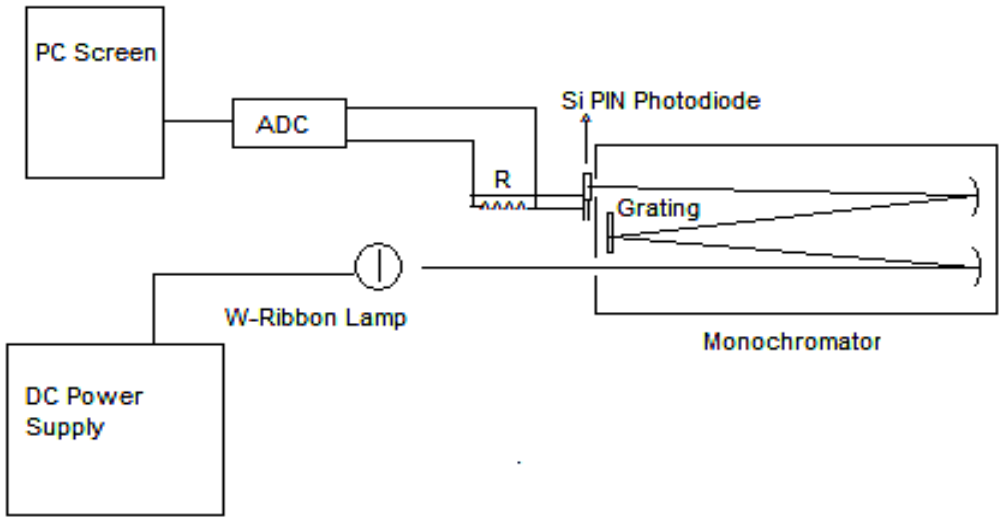

Figure 7 Scheme of setup

The resistance values have been chosen as 120 K and 265K for the outputsignal to be detectable by the ADC card and to have significant differences compared to noise between minima and maxima of the data. The resulting data was between 20mV-210mV with no significant sudden drops and consistent noise of maximum 3 mV showing excellent consistency between successive data sets.

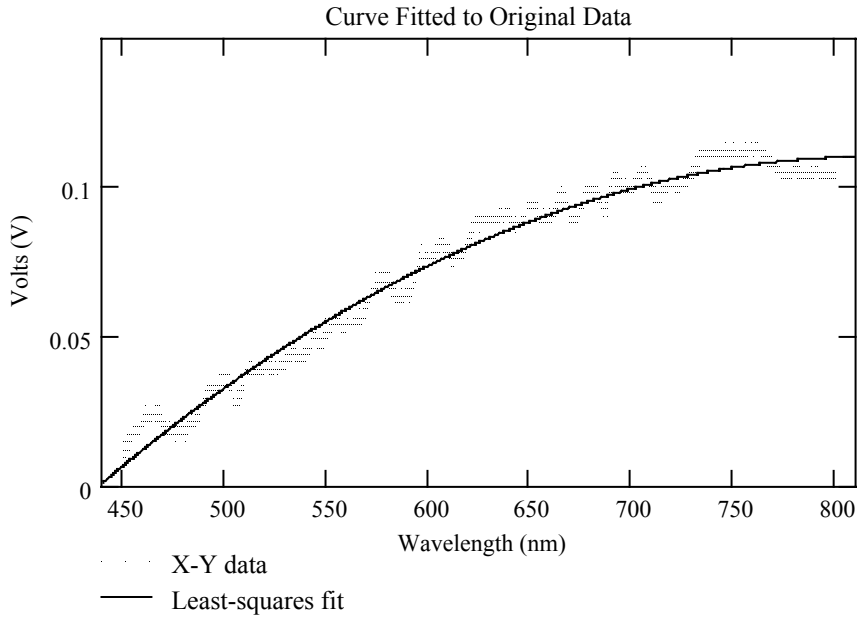

Figure 8 Data taken and fitted curve at 2600K with 120K resistance

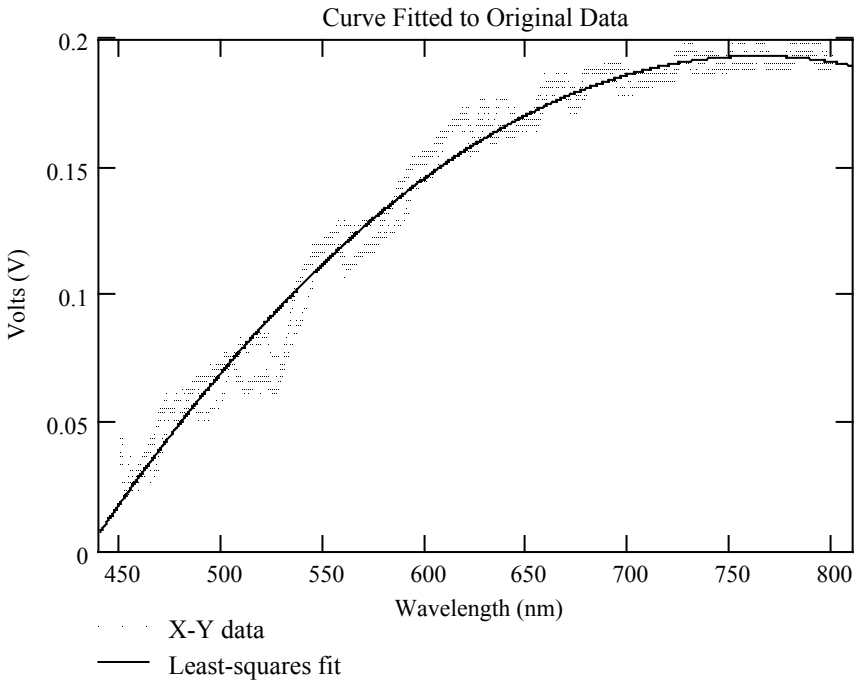

Figure 9 Data taken and fitted curve at 2600K with 265K resistance

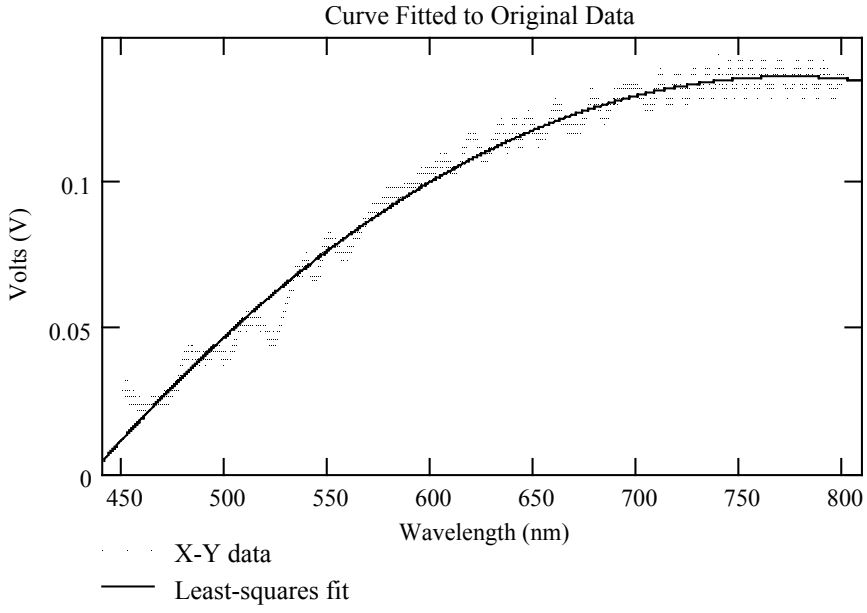

Figure 10 Data taken and fitted curve at 2700K with 120K resistance

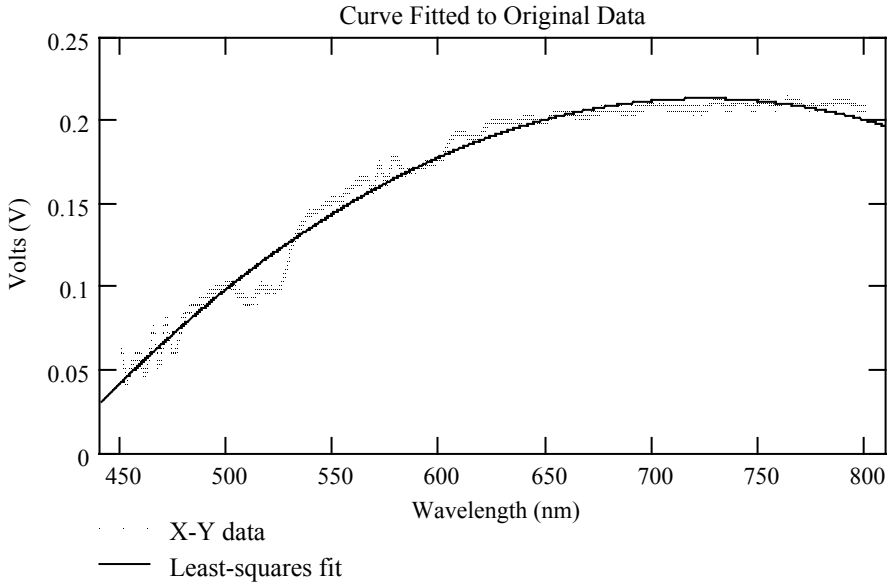

Figure 11 Data taken and fitted curve at 2700K with 265K resistance

Consequently the data sets of the final method were chosen for the evaluation of the system.

5.2.3 Spectral dependence of the absolute photon flux of the calibrated lamp:

The spectral radiant exitance with respect to wavelength of a blackbody with known temperature can be found using Plancks equation [7];

$$M_{\lambda} = \frac{3.745 \cdot 10^{8}}{\lambda^{5}} \frac{1}{e^{\frac{14388}{\lambda \cdot T}} - 1} \qquad \text{Eq.1}$$

Where the unit of M_{λ} is $W/m^2*\mu m$. Since our resolution is 3 nm we have to integrate Planck's equation in 3 nm intervals from 450nm to 800 nm for 2600K and 2700K to find the radiant exitance of a point souce for certain wavelengths [7];

$$M_{\lambda} = \int_{x_i}^{x_{i+1}} \frac{3.745 \cdot 10^{8}}{\lambda^{5}} \cdot \frac{1}{e^{\frac{14388}{\lambda \cdot T}} - 1} \cdot d\lambda \qquad \text{Eq.2}$$

Multiplying this result by the area of the tungsten filament gives us the radiant flux for certain wavelengths emitted by a blackbody the size of the tungsten filament; dividing by the spectral emissitivity gives us the radiant flux for certain wavelengths emitted by the tungsten filament. The ratio of those is given below:

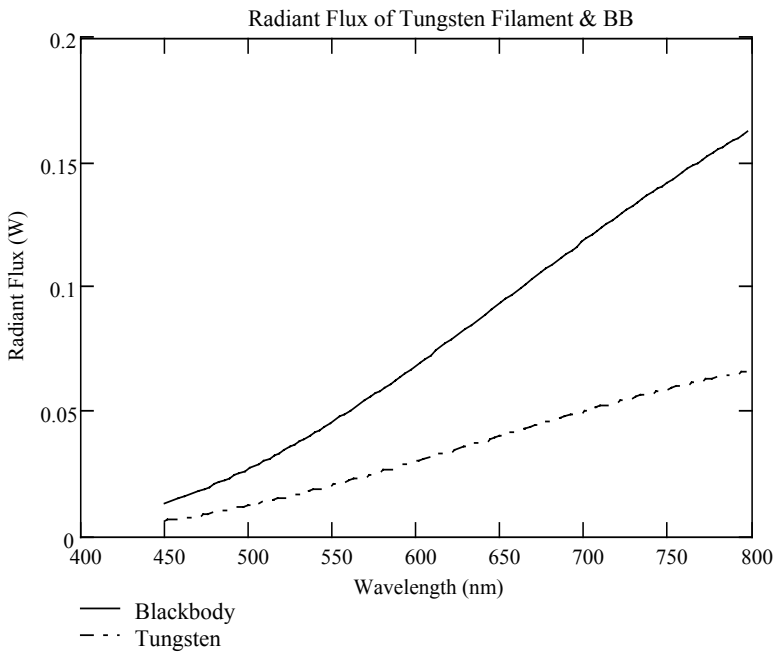

Figure 12 Radiant flux calculated for BB & Tungsten filament at 2600K

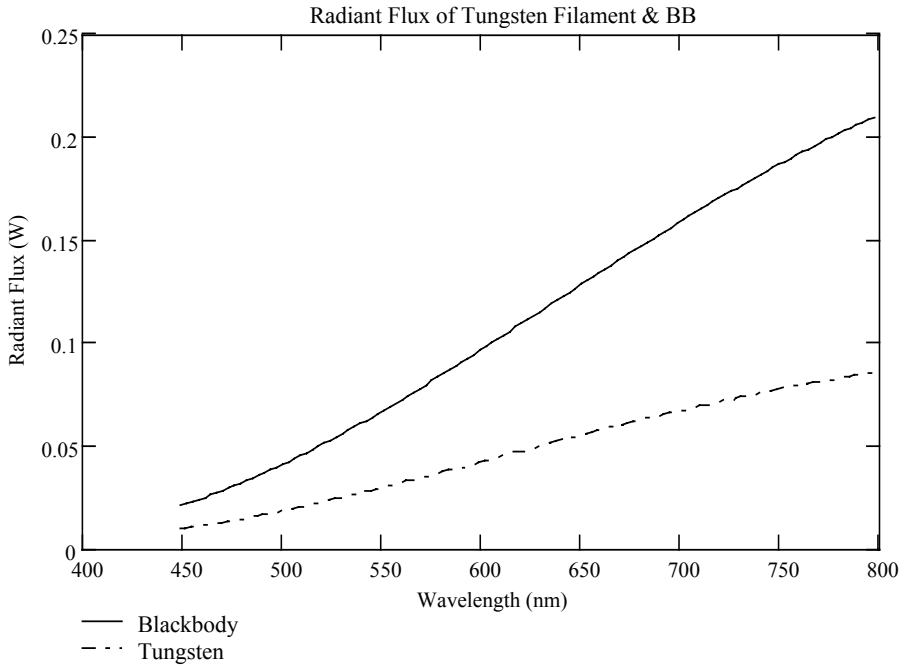

Figure 13 Radiant flux calculated for a BB & Tungsten filament at 2700K

Approximating the filament as a point source and multiplying the radiant flux by, the ratio of the area of the entrance slit to the surface area of a sphere with diameter 7 cm, gives us the radiant flux for certain wavelengths at the entrance slit;

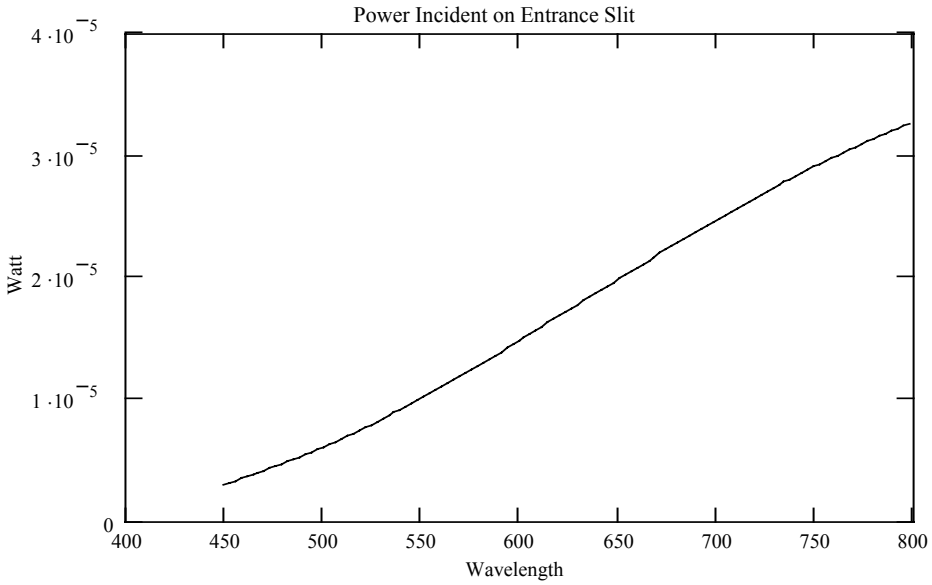

Figure 14 Power at Entrance Slit vs. Wavelength 2600K

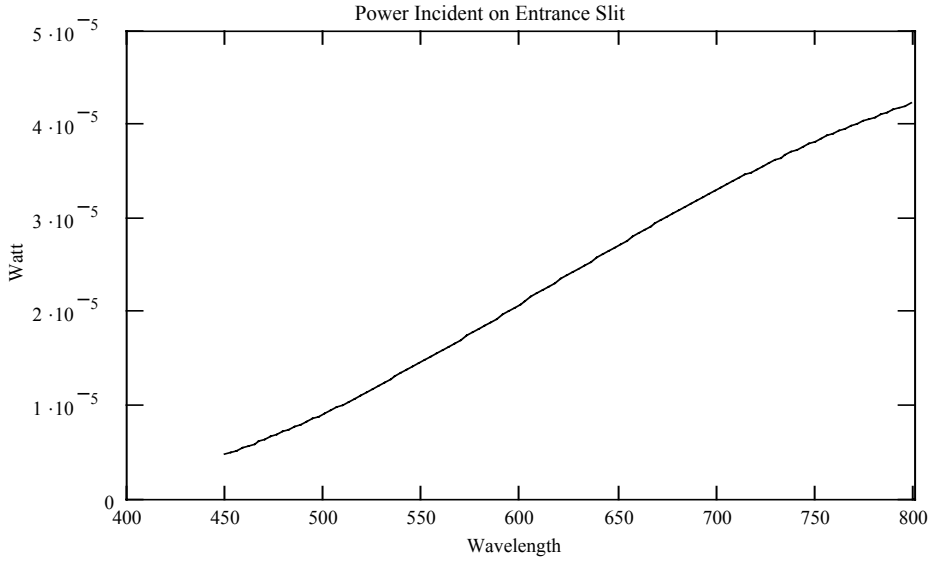

Figure 15 Power at Entrance Slit vs. Wavelength 2700K

Dividing the radiant flux at the entrance slit by the energy of a single photon at certain wavelengths results in the number of photons at the entrance slit;

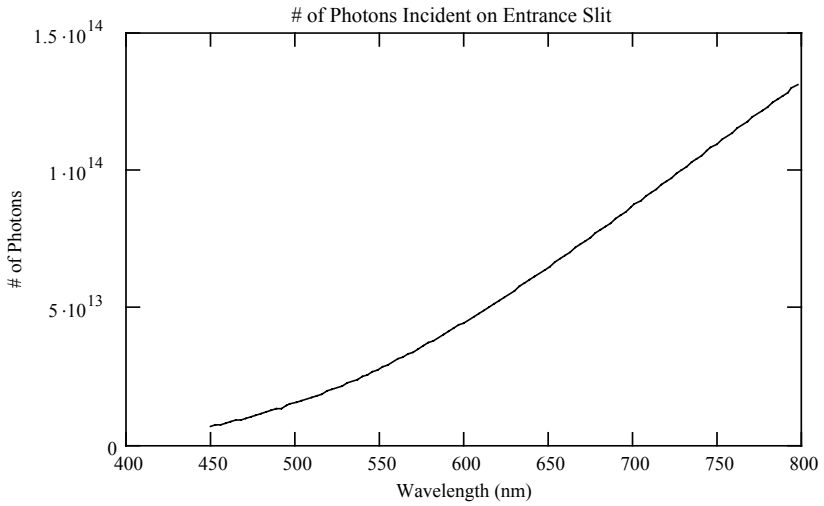

Figure 16 Number of photons at entrance slit vs. Wavelength 2600K

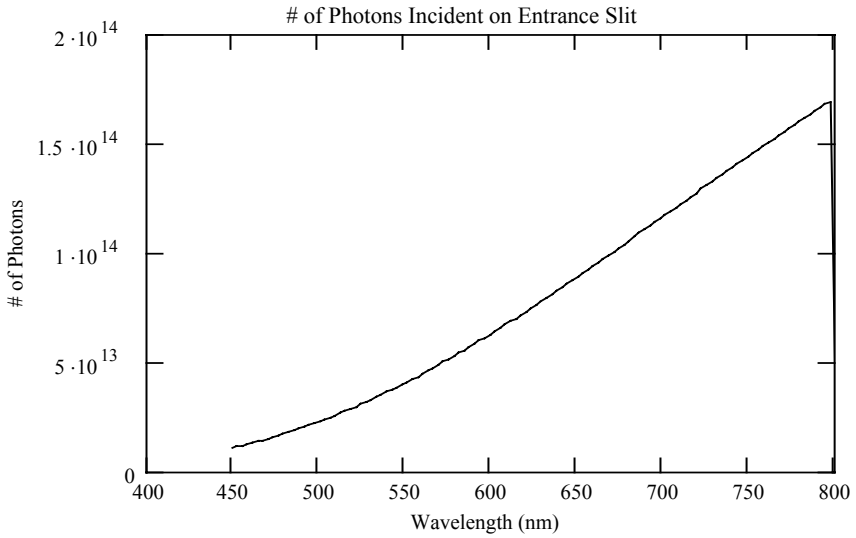

Figure 17 Number of photons at entrance slit vs. Wavelength 2700K

Which is the spectral dependence of the absolute photon flux of the calibrated lamp.

5.2.4 Calibration of the diode by comparison to the photon flux of the calibrated lamp:

Photo sensitivity is the ratio of radiant energy expressed in watts (W) incident on the device, to the resulting photocurrent expressed in amperes (A). Quantum efficiency is the photocurrent divided by the number of photons incident on the device. Since the measured quantity is V (Volts) in the setup instead of the photocurrent we have to replace V with A. Dividing V by the power at the entrance slit with respect to wavelength gives us a measure of the setups photo sensitivity. Dividing V by the number of photons at the entrance slit with respect to wavelength gives us a measure of the setups quantum efficiency. Although quantum efficiency is normally expressed in terms of the percentage of the incident photons which can be detected as a photocurrent, the fact that our data is in Volts leads to ridiculous values for the quantum efficiency of the system. The same can be said for the sensitivity of the system since the photosensitivity in A/W is generally in the 10^{-1} order.

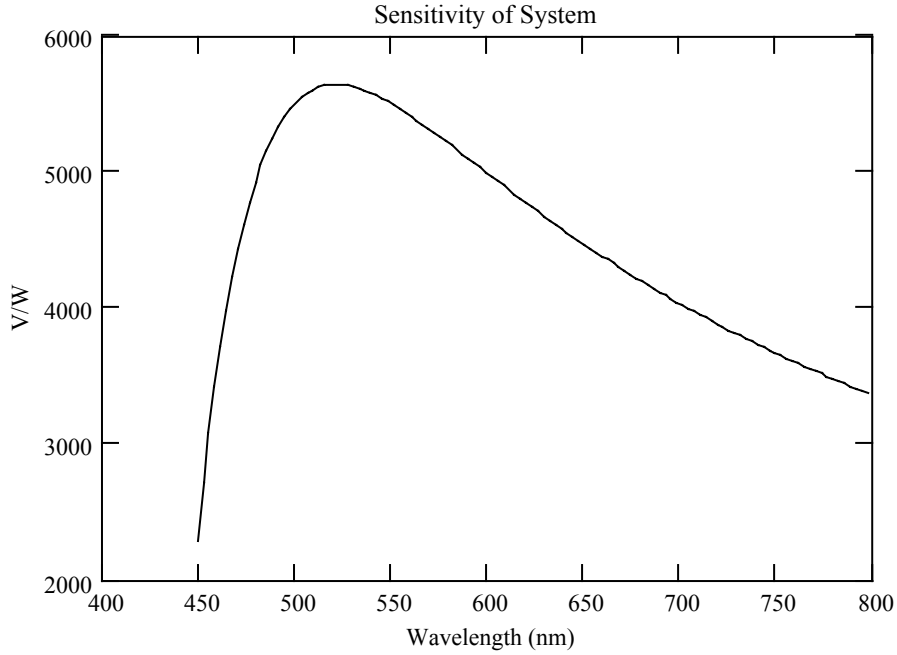

Figure 18 Sensitivity of system vs. Wavelength 2600K

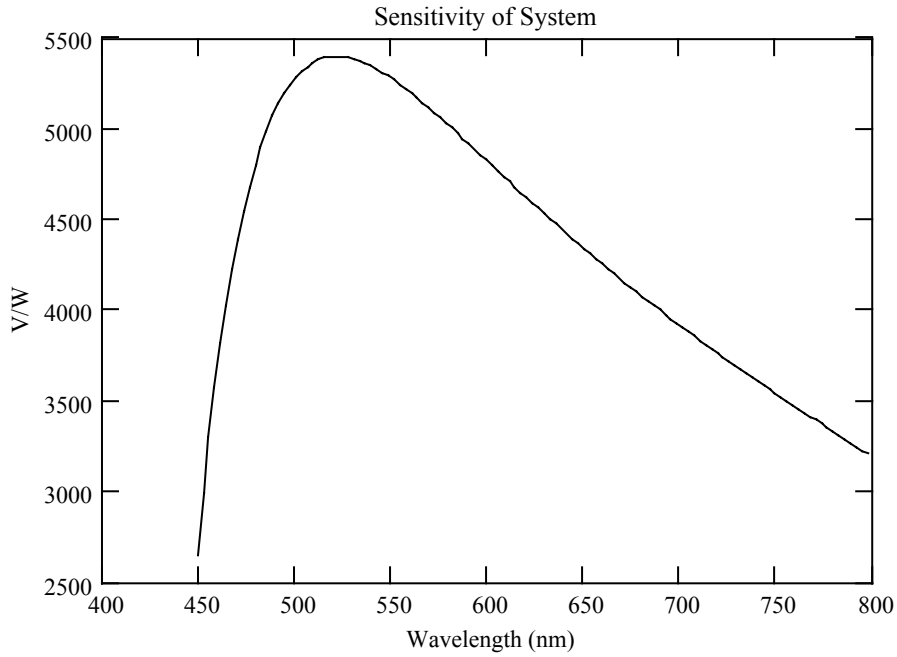

Figure 19 Sensitivity of system vs. Wavelength 2700K

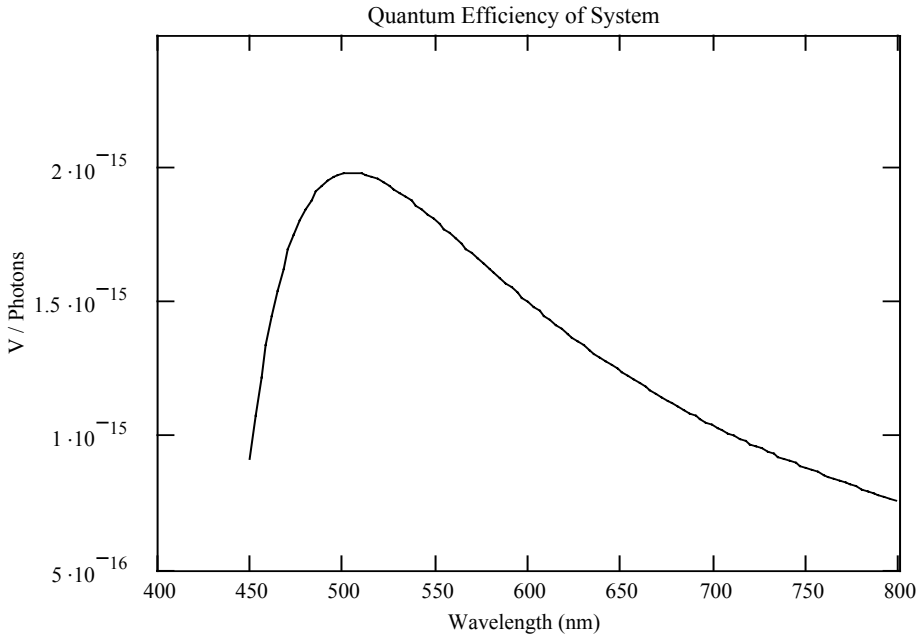

Figure 20 Quantum Efficiency of systemvs. Wavelength 2600K

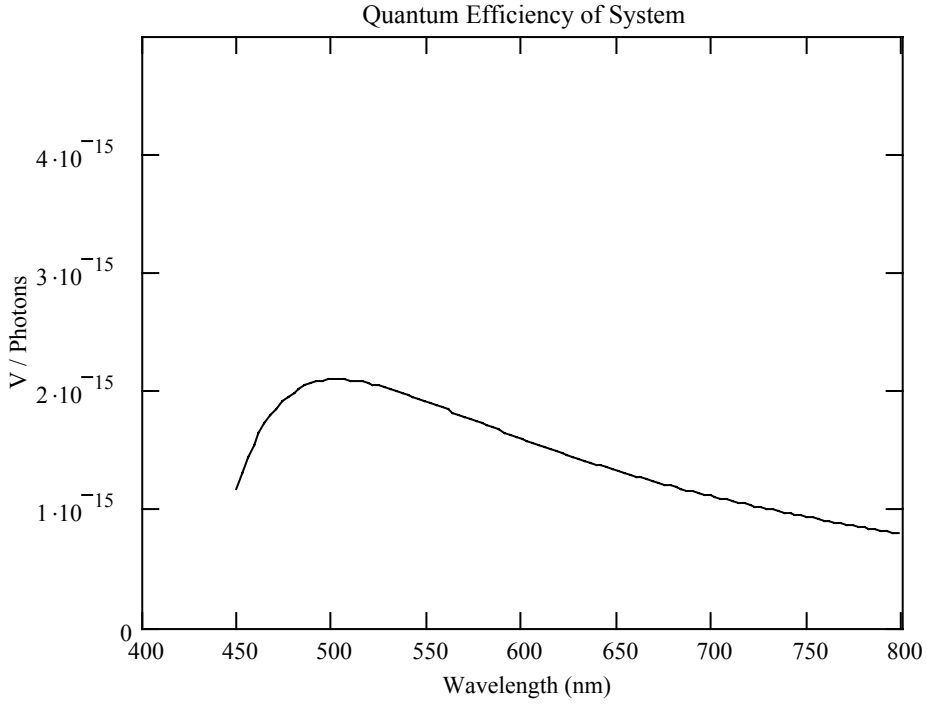

Figure 21 Quantum Efficiency of system vs. Wavelength 2700K

Since we have determined absolute radiant energy and absolute photon flux incident on the entrance slit, we should expect that the spectral sensitivity and the quantum efficiency do not vary with different ribbon temperature, meaning different radiant energy and absolute photon flux at same wavelength shouldn't affect spectral sensitivity and the quantum efficiency. Division of spectral sensitivity and the quantum efficiency for different ribbon temperatures should equal unity!

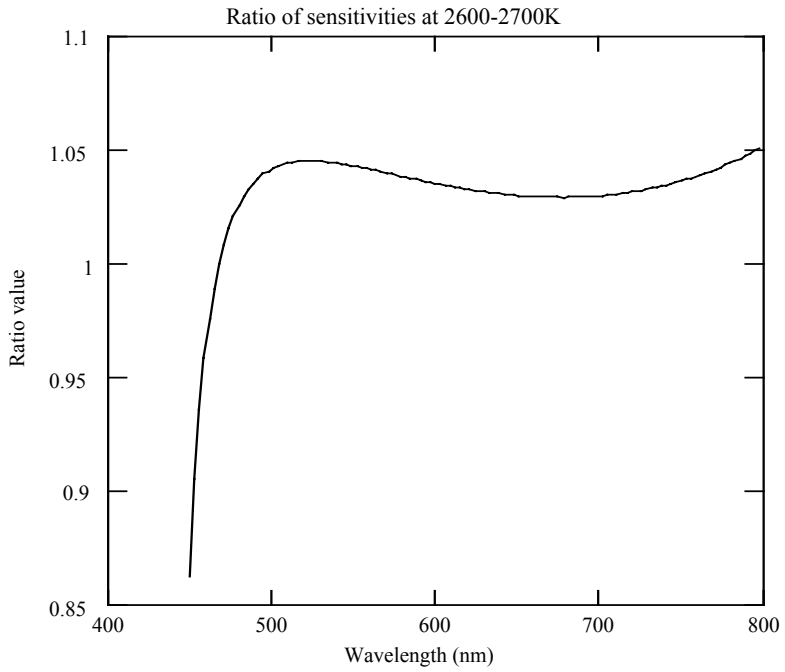

Figure 22 Ratio of sensitivities for 2600K-2700K vs. Wavelength

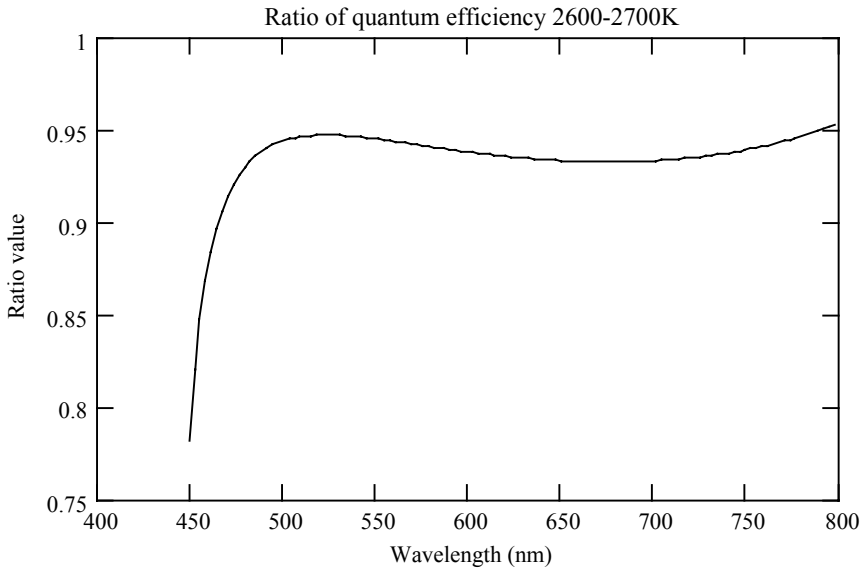

Figure 23 Ratio of quantum efficiencies for 2600K-2700K vs. Wavelength

As can be seen clearly above deviation from unity is observed. Possible reasons for this deviation will be discussed during the conclusion.

5.2.5 Determination of transmission and reflection coefficients:

The ratio of the measured curves with and without the optical component in front of the exit slit will give us simply the transmission coefficient of the component with respect to the wavelength from which we can deduce the reflection coefficient of the component with respect to the wavelength. For the data given below the optical component in front of the entrance slit is a piece of glass.

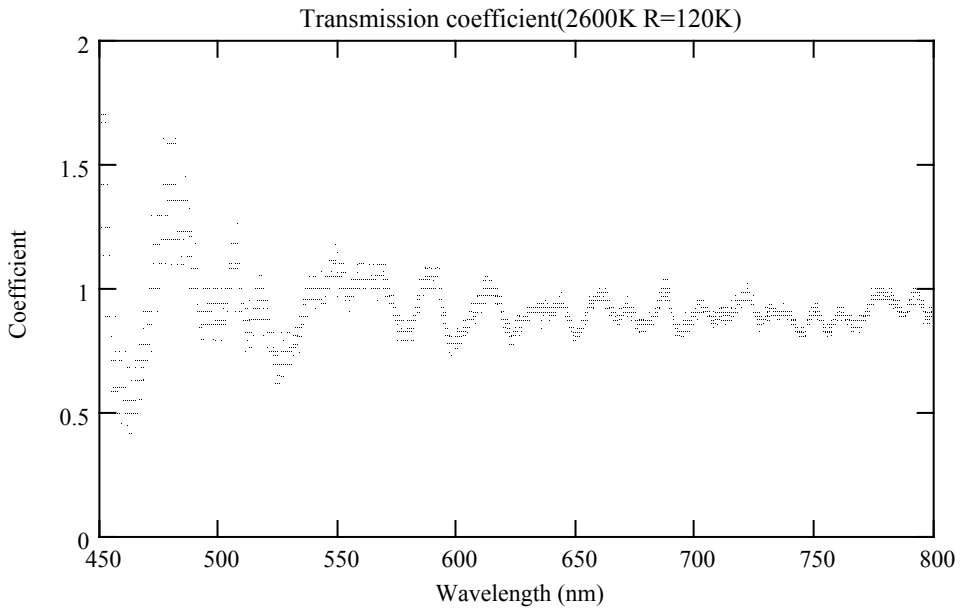

Figure 24 Transmission coefficients vs. Wavelength 2600K

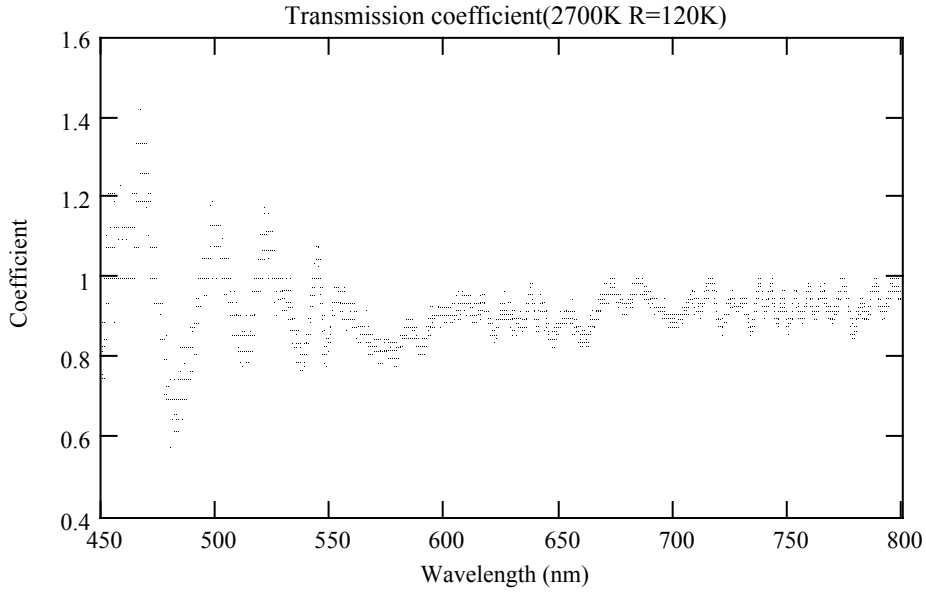

Figure 25 Transmission coefficients vs. Wavelength 2700K

Again a deviation from the expected result is observed since the ratio of transmission coefficients for different ribbon temperatures doesn't equal unity. Possible reasons for this deviation will be discussed during the conclusion.

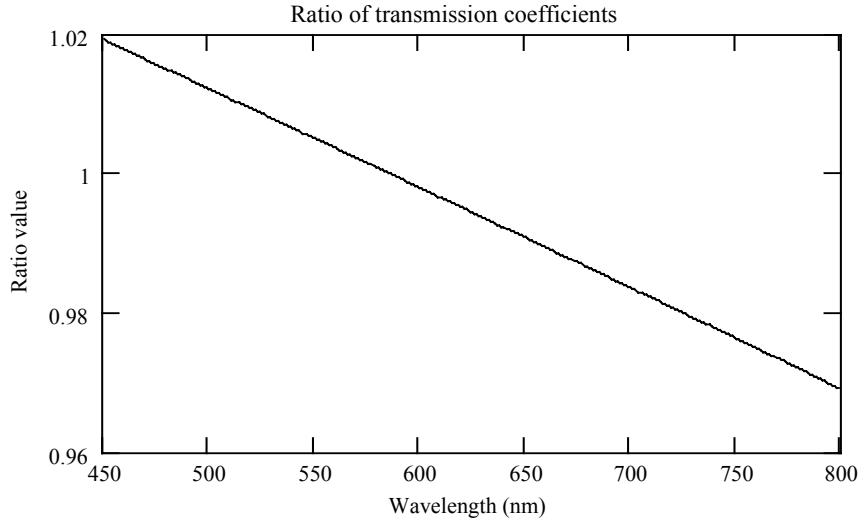

Figure 26 Ratio of transmission coefficients at 2600K-2700K vs. Wavelength

CHAPTER 6
CONCLUSIONS

The design, assembly and calibration of an optical setup that allows the determination of the transmission and reflection coefficients of optical components within the wavelength range from 450nm to 800nm which was the main purpose is achieved. Consequent errors result from the resolution of the monochromator nearly equalling 1.5 nm for full slitwidth, the sensitivity of the ADC card which can only be calibrated down to the mV range, the apparent incompatibility between the diode and the ADC card, the lack of a device able to measure the diodes output in terms of Amperes since the outputcurrent is in the range of nA, the multiplication of noise because of the large resistance attached to the diode, deposited tungsten on the inner bulb surface which can decrease the flux output by as much as %18, the relative low transmittance of the glass bulb of the tungsten strip lamp below 400nm, dark current of the photodiode, stray light contribution, the attenuation of radiant flux by air and order effects.

The lack of the efficiency curves of the gratings is a serious issue and the spectral sensitivity and quantum efficiency curves have to be modified according to these curves. The spectral sensitivities of all photodiodes are increasing in the 450-800 nm range whereas the spectral sensivity of the system evaluated with the data at hand is decreasing in the 450-800 nm range which can only be explained by the fact that the efficiency curves of the gratings should exhibit a steep decrease in that very same range.

The experimental setup which consisted of the Jarrell-Ash Ebert type scanning monochromator, the Hamamatsu Si PIN Photodiode, a PC connected ADC card, the Osram tungsten strip lamp and a power supply for the lamp was successfully assembled. The different parts needing calibration were calibrated with calibration techniques suitable for our purposes and connected to the system

in a proper way. The setup is best suited to carry out spectral response calibrations and transmission coefficient measurements.

Transmission measurements and spectral response calibration were carried out and the experimental results showed some deviation from the theoretical predictions. The most serious deviations are in the 450nm-500nm range where there is also a more rapid increase in diodeoutput compared to other regions. Considering this fact together with the higher noise/signal ratio in this region and the apparent increase in sensitivity and quantum efficiency ratios for different temperatures in this region, the only conclusion we can draw is that our system is best suited for measurements above 500nm. The analysis above 500 nm of the spectral sensitivities, quantum efficiencies and the ratios of those for different ribbon temperatures suggests that our system, when keeping in mind the number of factors contributing to the accuracy of the system, works in a reasonable error range. The ratio of spectral sensitivity shows a maximum deviation of .05 from 1 equalling an error of %5 which can be explained with the factors contributing to the error. The ratio of quantum efficiency shows a maximum deviation of .07 from 1 equalling an error of %7 which also can be explained with the factors contributing to the error. The spectral sensitivity for the ribbon temperature 2600K is greater than that for 2700K through the whole 500nm-800nm range whereas the quantum efficiency for the ribbon temperature 2700K is greater than that for 2600K through the whole 500nm-800nm range. Which means that the quantum efficiency and the spectral sensitivity are both dependent on the number of incident photons on the active area of the photodiode, since at fixed wavelength the only difference between ribbon temperature 2600K and 2700K is the number of photons emitted to compensate for the difference of radiant exitances for different temperatures, which they shouldn't be since we divide by number of photons to evaluate the quantum efficiency and by radiant exitances to evaluate the spectral sensitivity. The missing efficiency curves of the gratings can't explain this phenomen since they are independent of incident light. Possible reason for this discrepancy maybe that one or several of the factors which are assumed to be contributing linearly with respect to incident light intensity is a function of

incident light intensity or that one of the several approximations made in evaluating absolute photon fluxes bears such a factor.

The biggest obstacles in front of more accurate measurements were the lack of time and a device able to measure the diodeoutput in terms of Amperes which would eliminate all the errors stemming from the ADC card, which has proven itself to be unreliable when compared to other means of measurement, but had to be used inevitably since it provides the best option for keeping track and recording the data. Other improvements to the system can be made by interchanging the various parts of the setup like the monochromator, the ADC card and analyzing the effect of various factors contributing to the error more closely and even including the evaluation of different factors which are neglected in the calculations. The evaluation of an attenuation factor with respect to incident light intensity, for the spectral sensitivity and the quantum efficiency of the whole setup, presents itself as the most obvious solution in order to achieve absolute spectral response calibration.

REFERENCES

1. Brown, Steven D., Computer Assisted Analytical Spectroscopy, Chichester; New York: Wiley, c1996

2. George, A. Vanasse, Spectrometric Techniques, Academic Press, 1977

3. Austerlitz, Howard, Data Acquisition Techniques Using Personal Computers, Academic Press, 1991

4. Buchanan, William, Applied PC Interfacing, Graphics and Interrupt, Addison Wesley Longman, 1986

5. Diefenderfer, A.James, Principles of Electronic Instrumentation, W.B.Saunders Comp, 1979

6. Levi, Leo, Applied Optics: A guide to Optical System Design, John Wiley and Sons, 1968

7. Pedrotti, Frank L., Introduction to Optics, Prentice-Hall International, 1993

8. Jenkins, Francis A., Fundamentals of Optics, New York, McGraw-Hill, 1957

9. Jerry Workman Junior, Art W. Springsteen, Applied Spectroscopy, Academic Press, c1998

10. McGucken William, 19th Century Spectroscopy, Development of Understanding Spectroscopy, Johns Hopkins Press [c1969

11. Allan Billings, Optics, Optoelectronics and Photonics, Prentice Hall, 1983

12. Hetch, Eugene, Optics, Addison-Wesley Pub. Co. 1974

13. Optical Society of America, Handbook of Optics, McGraw-Hill, 2001

14. Mark, Howard, Principles and Practice of Spectroscopic Calibration, J. Wiley, c1991

15. Dolan, Thomas James, Fusion Research: Principles, Experiment ant Technology, Pergamon Press, c1982

16. Hamamatsu Optical Instruments Catalog, 2001

17. Jarrel-Ash MonoSpec-50 Catalog, 1983

18. Improvement to monochromator spectral calibration using a tungsten strip lamp, Hannspeter Winter and E.W.P. Bloemen, J.Phys. E: Sci. Instrum Vol.15, 1982
19. Simple designs to measure efficiency of different type of monochromators, O.Prakash, R.S. Ram, J.Optics (Paris), Vol.27. 1996, pp 241-245
20. Effect of the geometrical parameters on an absolute calibration, J.P.Lanquart, J.Phys D: Appl. Phys 19 (1986),pp 2043-2049
21. Simple method of spectrometer-detector sensitivity calibrations in the 210-1150nm range, A.A. Fataev, E.H.Fint, A.M. Pravilov, Meas. Sci. Technology, 10 (1999), pp 182-185

APPENDIX

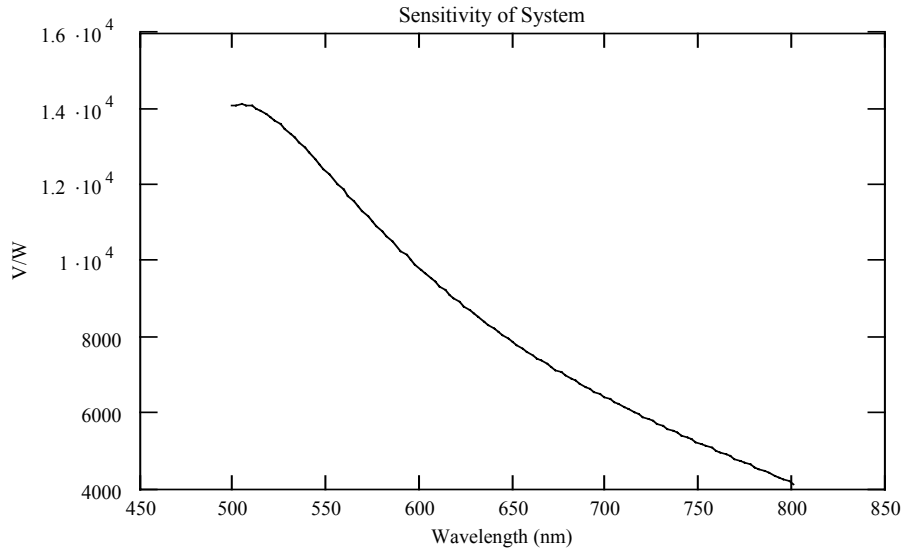

Figure A.1: Sensitivity with S1133-14 Diode at 2700K with R=265K

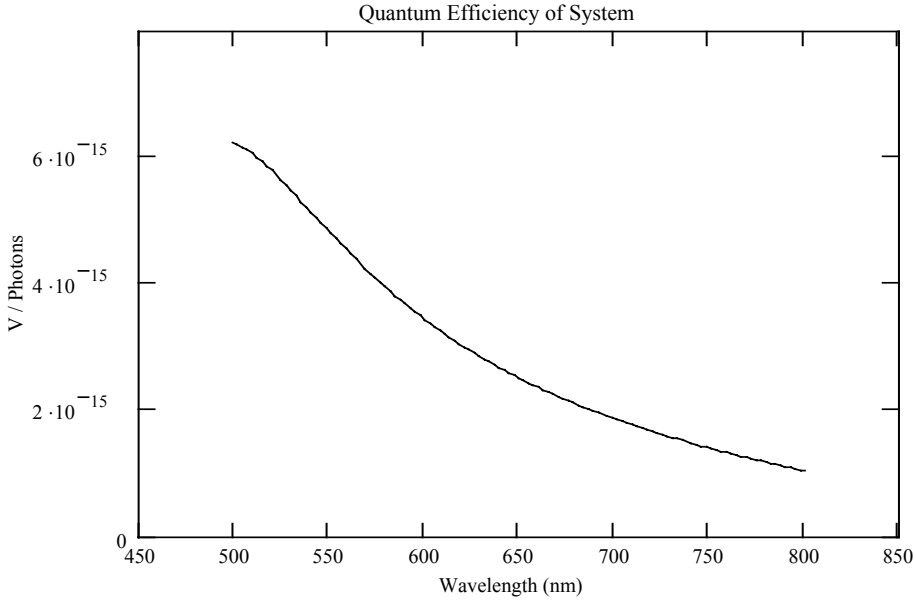

Figure A.2: Quantum efficiency with S1133-14 Diode at 2700K with R=265K

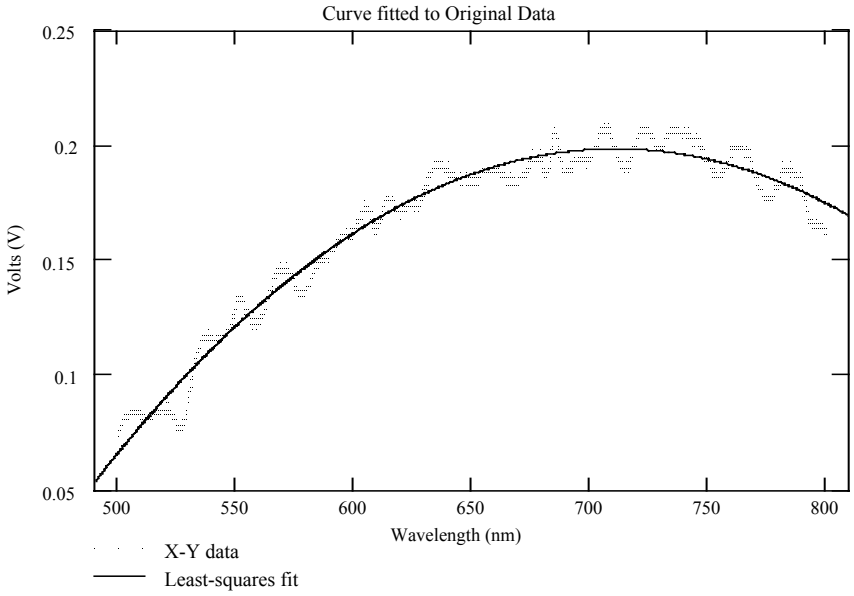

Figure A.3: Data and curve fitted with S1133-14 Diode at 2700K with R=265K

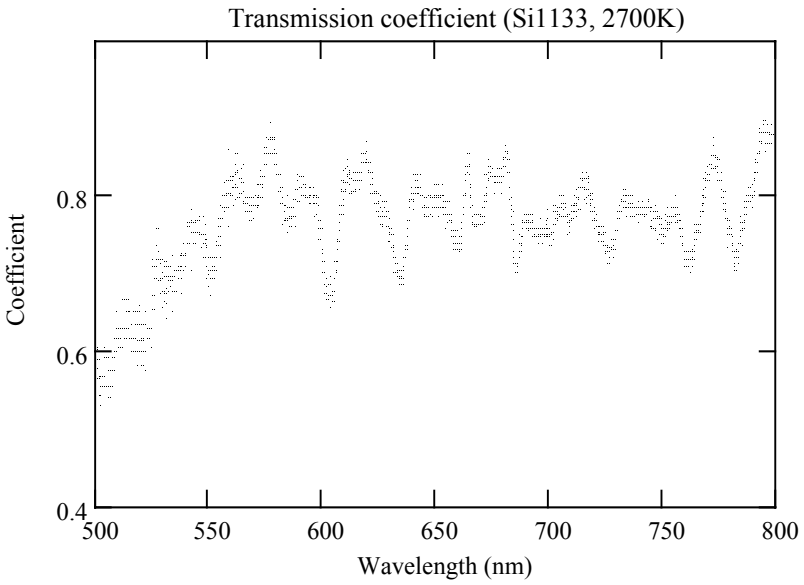

Figure A.4: Transmission coefficient with S1133-14 Diode at 2700K (R=265K)

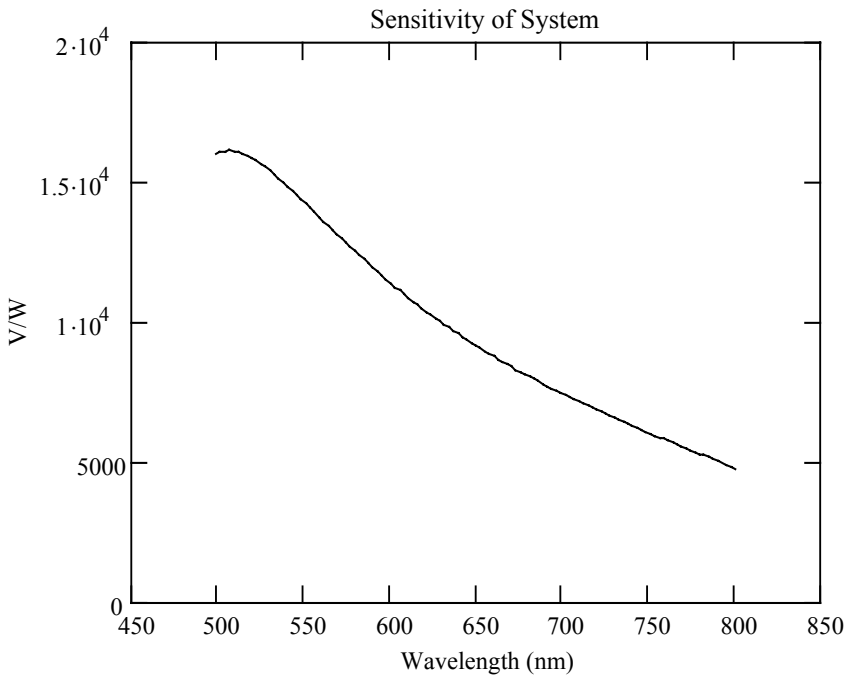

Figure A.5: Sensitivity with S1227-33BQ Diode at 2700K with R=265K

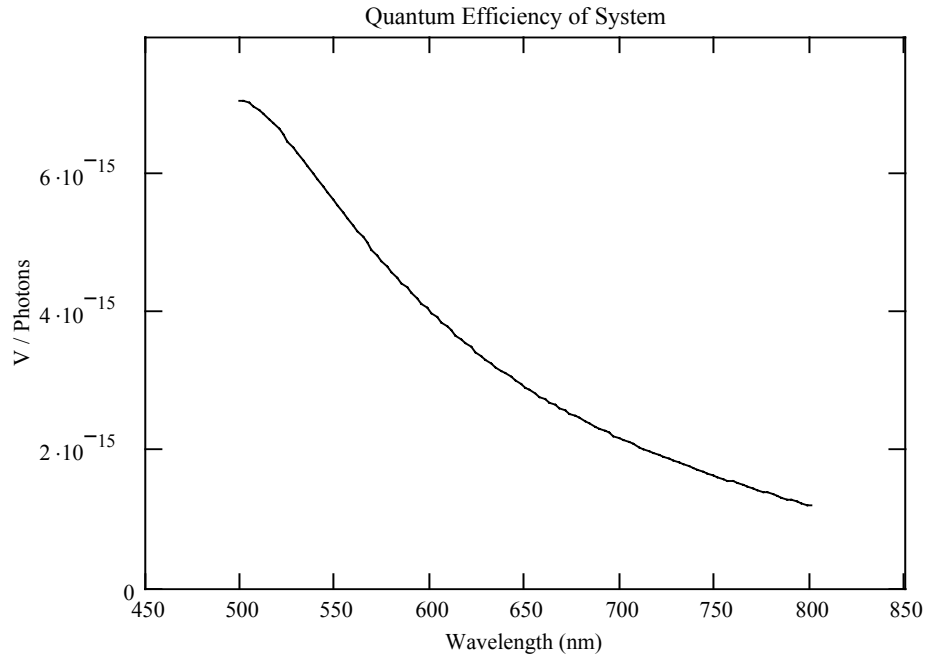

Figure A.6: Quantum efficiency with S1227-33BQ Diode at 2700K (R=265K)

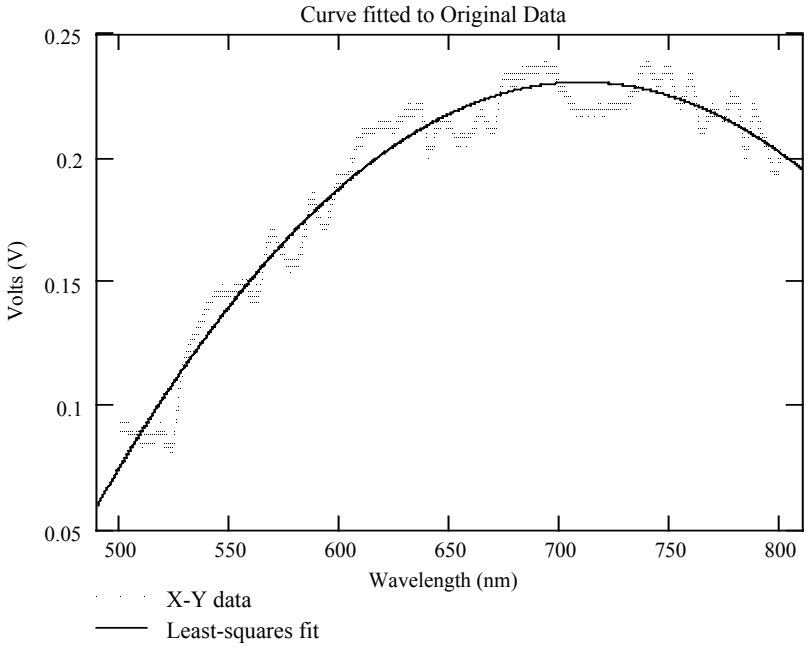

Figure A.7: Data and fitted curve with S1227-33BQ Diode at 2700K (R=265K)

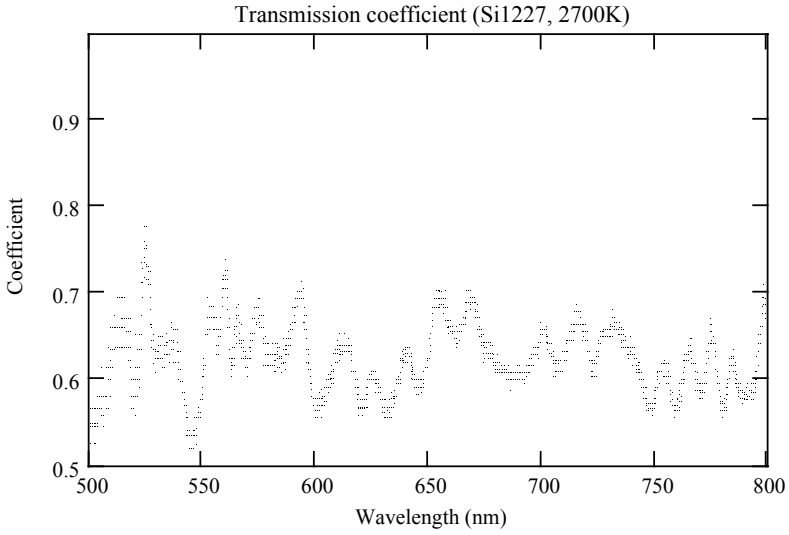

Figure A.8: Transmission coefficient with S1227-33BQ Diode at 2700K (R=265K)

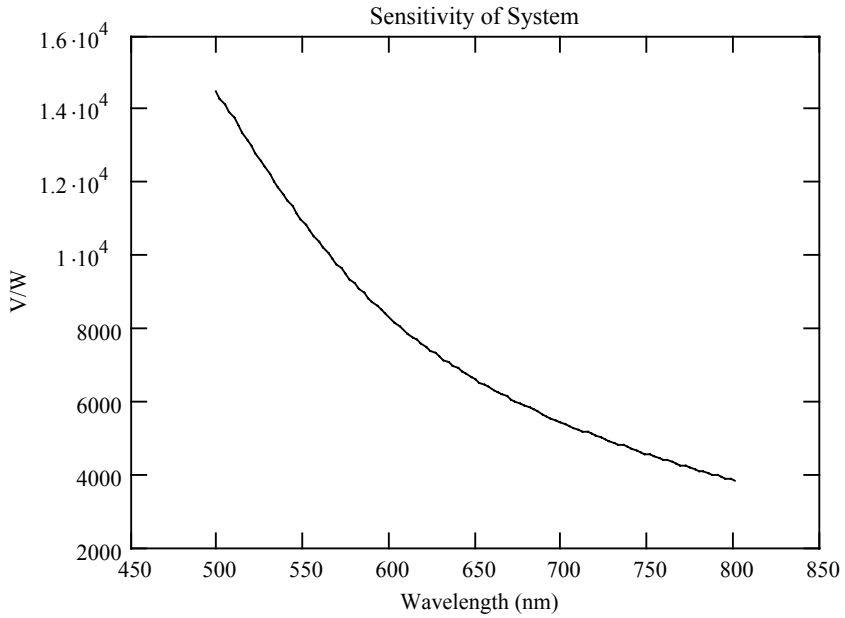

Figure A.9: Sensitivity with Monospec50 and S1133-14 Diode at 2700K

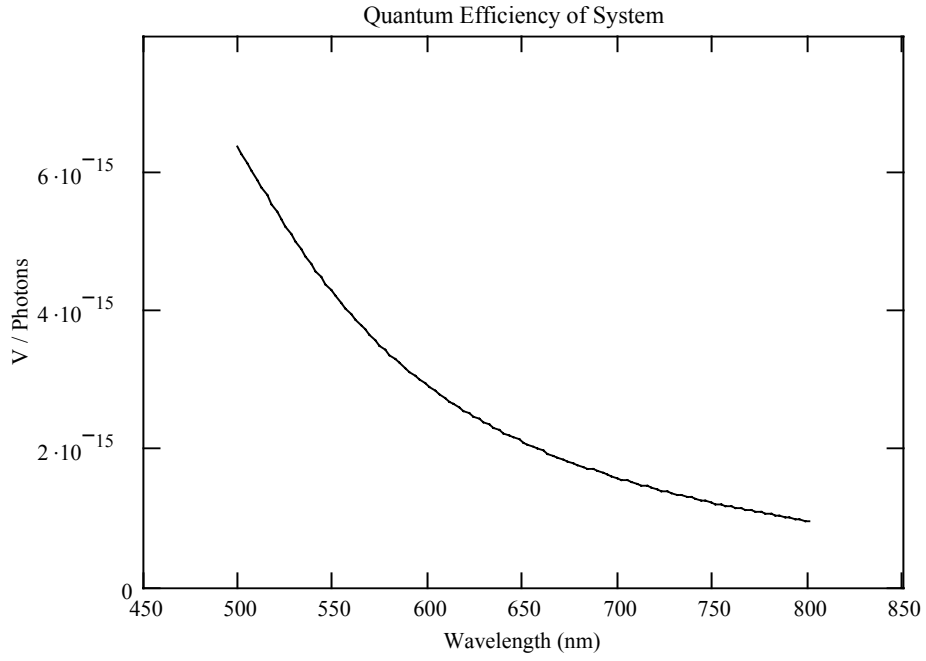

Figure A.10: Quantum efficiency with Monospec50 and S1133-14 Diode at 2700K

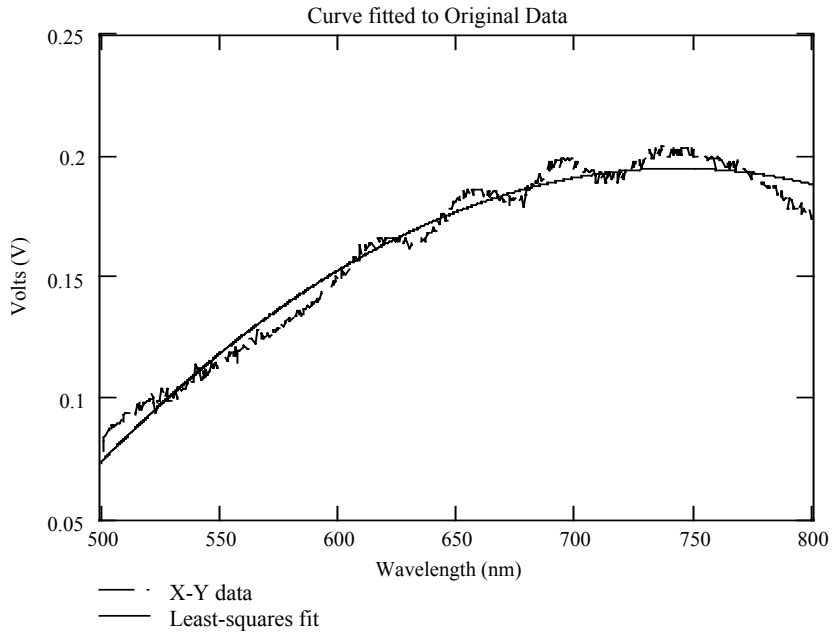

Figure A.11: Data and curve fitted with Monospec50 and S1133-14 Diode at 2700K

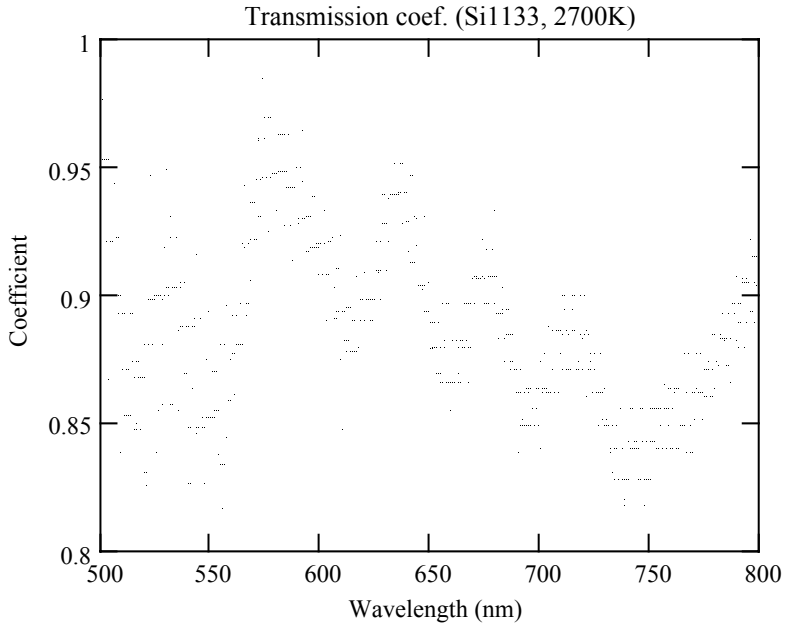

Figure A.12: Transmission coefficient with Monospec50 and S1133-14 Diode at 2700K

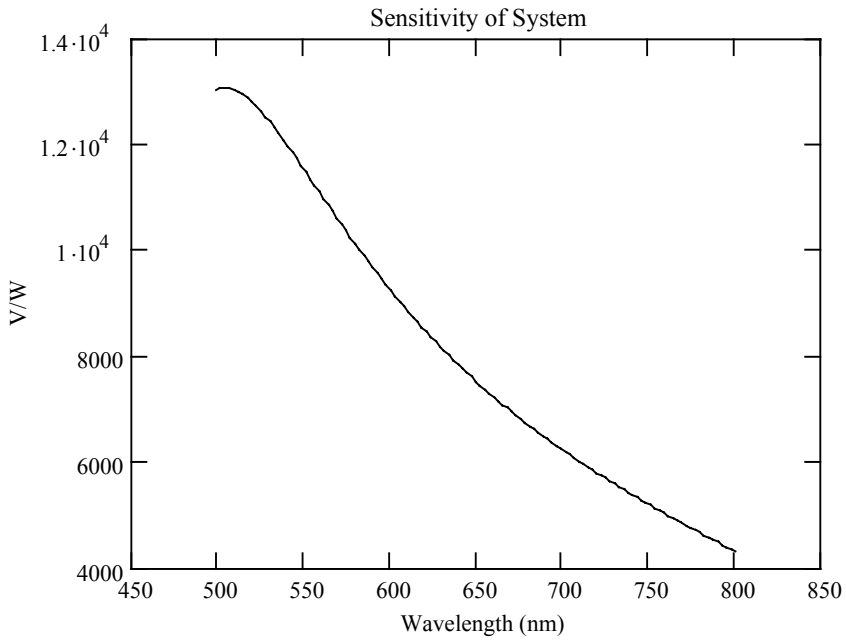

Figure A.13: Sensitivity with Monospec50 and S1227-33BQ Diode at 2700K

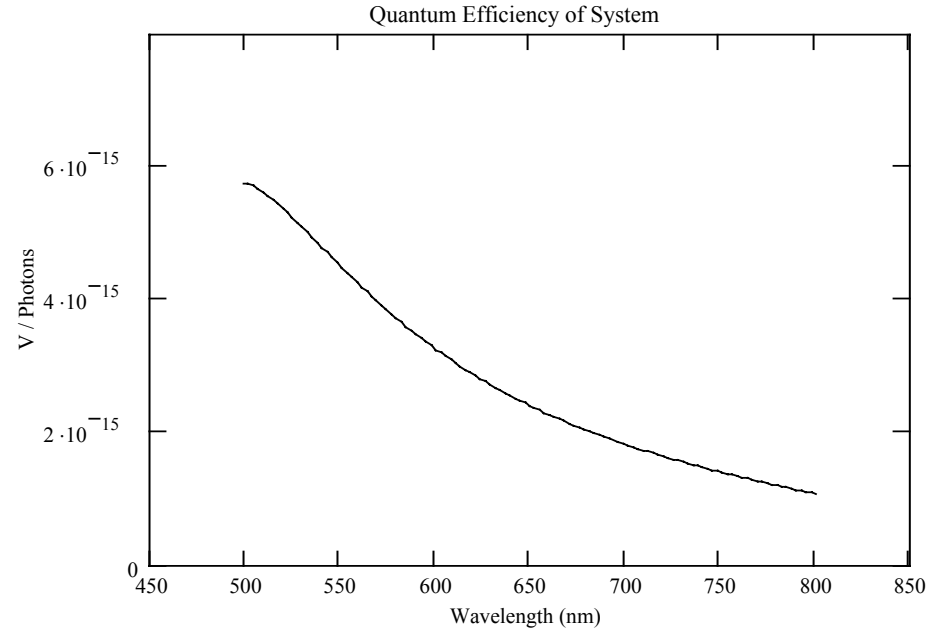

Figure A.14: Quantum efficiency with Monospec50 and S1227-33BQ Diode at 2700K

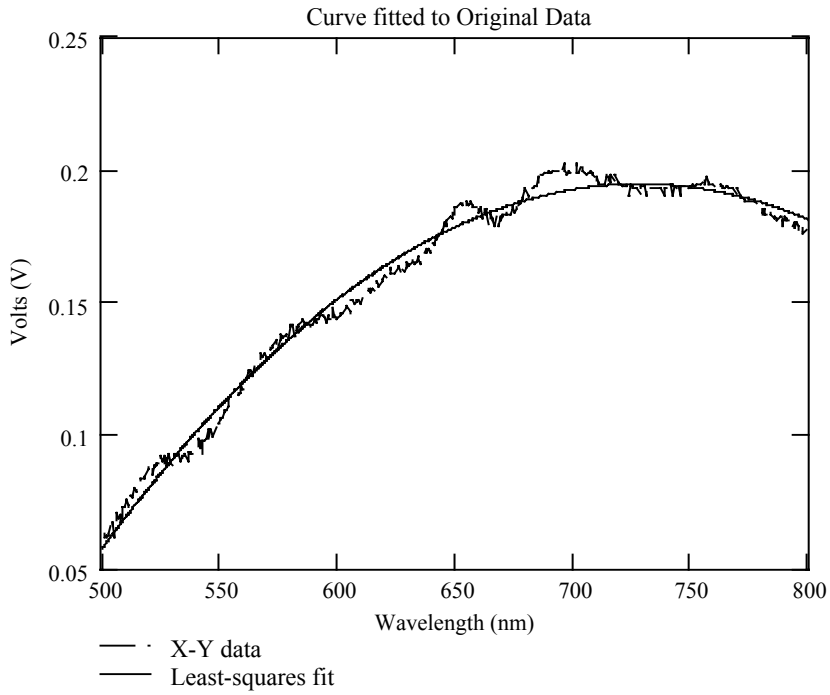

Figure A.15: Data and curve fitted with Monospec50 and S1227-33BQ Diode at 2700K

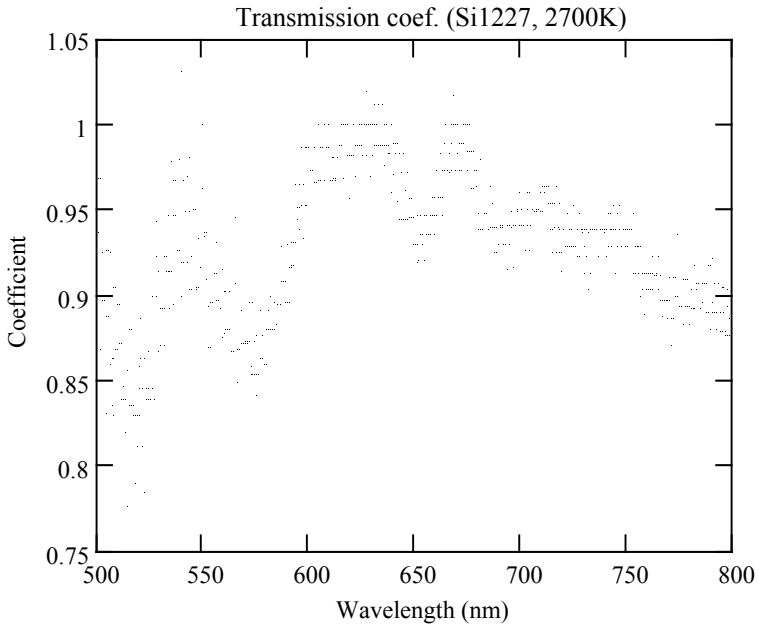

Figure A.16: Transmission coefficient with Monospec50 and S1227-33BQ Diode at 2700K